AWARD NUMBER: W81XWH-13-1-0482

TITLE: Treatment of Neuropathic Pain after SCI with a Catalytic Oxidoreductant

PRINCIPAL INVESTIGATOR: Candace L. Floyd, Ph.D.

CONTRACTING ORGANIZATION:
University of Alabama at Birmingham
Birmingham AL, 35249-7330

REPORT DATE:
October 2014

TYPE OF REPORT:
Annual

PREPARED FOR: U.S. Army Medical Research and Materiel Command
                            Fort Detrick, Maryland 21702-5012

DISTRIBUTION STATEMENT: Approved for Public Release;
                                        Distribution Unlimited

The views, opinions and/or findings contained in this report are those of the author(s) and should not be construed as an official Department of the Army position, policy or decision unless so designated by other documentation.

REPORT DOCUMENTATION PAGE

1. REPORT DATE	2. REPORT TYPE	3. DATES COVERED
October 2014	Annual	30 Sep 2013 - 29 Sep 2014

4. TITLE AND SUBTITLE
Treatment of Neuropathic Pain after SCI with a Catalytic Oxidoreductant

5a. CONTRACT NUMBER

5b. GRANT NUMBER
W81XWH-13-1-0482

5c. PROGRAM ELEMENT NUMBER

6. AUTHOR(S)
Candace L. Floyd, Ph.D.

E-Mail:clfloyd@uab.edu

5d. PROJECT NUMBER

5e. TASK NUMBER

5f. WORK UNIT NUMBER

7. PERFORMING ORGANIZATION NAME(S) AND ADDRESS(ES)
University of Alabama at Birmingham
Spain Rehabilitation Center Room 529
1717 6th Avenue South
Birmingham AL, 35249-7330

8. PERFORMING ORGANIZATION REPORT NUMBER

9. SPONSORING / MONITORING AGENCY NAME(S) AND ADDRESS(ES)

U.S. Army Medical Research and Materiel Command

Fort Detrick, Maryland 21702-5012

10. SPONSOR/MONITOR'S ACRONYM(S)

11. SPONSOR/MONITOR'S REPORT NUMBER(S)

12. DISTRIBUTION / AVAILABILITY STATEMENT

Approved for Public Release; Distribution Unlimited

13. SUPPLEMENTARY NOTES

14. ABSTRACT
The on-going research is to test the central hypothesis that post-SCI administration of the catalytic oxidoreductant BuOE will inhibit neuropathic pain after SCI. The research in year 1 focused on the goal of aims 1 and 2, to test the hypothesis that post-SCI administration of BuOE decreases inflammation and ROS activation in a rat and mouse model of SCI. The main finding of our work in this year was to evaluate the dose-effect curve of post-SCI administration of BuOE on the outcomes listed above. Our data from on-going experiments indicate that the dose of 0.1mg/kg BuOE was most effective in reducing inflammation and ROS activation acutely post-SCI in rats and mice. On-going experiments will evaluate additional outcome measures and behavioral outcomes in the subsequent year.

15. SUBJECT TERMS nothing listed

16. SECURITY CLASSIFICATION OF:			17. LIMITATION OF ABSTRACT	18. NUMBER OF PAGES	19a. NAME OF RESPONSIBLE PERSON USAMRMC
a. REPORT Unclassified	**b. ABSTRACT** Unclassified	**c. THIS PAGE** Unclassified	Unclassified	34	**19b. TELEPHONE NUMBER** *(include area code)*

Table of Contents

1. INTRODUCTION:

Although the neurobiological mechanisms that underlie neuropathic pain are poorly understood, we hypothesize that a highly efficacious treatment for neuropathic pain after SCI would be a molecule that scavenges ROS, inhibits NF-κB activation, is bioavailable to the CNS, and is well tolerated. We have extensive experience in the development of a class of therapeutic catalytic oxidoreductants which *both* dissipate ROS *and* inhibit NF-κB activation. Thus, the objective of this research is to evaluate MnTnBuOE-2-PyP^{5+} (BuOE2) as a novel therapeutic to treat neuropathic pain after SCI as it offers the unique and simultaneous chemistry of direct redox-regulation of pro-inflammatory promoting signaling pathways and dissipation of ROS. The proposed research will test the central hypothesis that post-SCI administration of the catalytic oxidoreductant BuOE2 will inhibit neuropathic pain after SCI by assessing the effects of post-SCI administration of BuOE2 on ROS, NF-κB signaling, inflammation, and pain-associated behaviors in a clinically relevant *rat* model of *cervical contusion* SCI and a *mouse* model of *ischemic* SCI (Aims 1 and 2). The experiments of efficacy in rodent models will then be followed up in a large animal model of SCI, the porcine contusion model (Aim 3).

2. KEY WORDS:

Neuropathic pain, spinal cord injury, reactive oxygen species, cervical contusion, ischemic spinal cord injury, oxidative stress, inflammation

3. ACCOMPLISHMENTS

Major Goals of the Project in Year 1:

The year 1 major goals/ deliverables were to:
- **Perform pharmacokinetic analysis of subcutaneous BuOE2 in both rats and mice**
  We have successfully completed this goal and determined the PK for administration of BuOE2 in rats in mice. Parts of these data are included in the manuscript by Tovmasyan et al, submitted to ReDox Biology (appendix 1). Other data are included under the details per task section below.

- **Determine the dose of BuOE2 that is most effective in reduction ROS, inhibiting NF-kB signaling, and inflammation in the spinal cord acutely post-SCI**
  We have completed approximately 70% of the experiments in support of this goal and anticipate full completion by March 2015. Thus far, the main finding is that the 0.1mg/kg dose is seemingly the most effective in reducing ROS and inflammation after SCI in the rodent models. Please see the data included under the details per task section, below.

- **Disseminate data concerning above to the medical and scientific community by publication in peer-reviewed journal and presentation at national meetings.**

  As described above, the group submitted 1 manuscript (appendix 1). We anticipate another manuscript on these data will be submitted by June 2015.

Accomplishments by the Specific Objectives of the SOW for Year 1:

Task 1: Obtain required regulatory approval for project, including IACUC, Occupational Health Approval, and ACURO from UAB (Floyd and Tse) and from Duke (Warner, Batinic-Haberle, Spasojevic, Sheng). Months 1-3.

This goal was achieved by IACUC ACURO approval completed by February 2014.

Task 2: Quantitatively assure purity of sufficient BuOE2 for use at both UAB and Duke for Year 1 *in vivo* studies. Order all necessary surgical supplies and biochemistry/ molecular reagents (ALL). Months 1-12.

This goal was achieved. Purity of the compound was ensured by February 2014 and the research teams obtained necessary supplies to conduct the experiments detailed below.

Task 3: Order and acclimate adult male rats for evaluation in acute post-SCI time points related to Aim 1 at UAB (Floyd). Order and acclimate adult male mice and rats for BuOE2 subcutaneous pharmacokinetic studies (Warner and Spasojevic). Order and acclimate adult male mice for evaluation in acute post-spinal cord ischemia time points related to Aim 2 at Duke (Warner and Sheng). Months 3-12.

This goal was achieved and the data obtained from these animals are detailed below with other tasks.

Task 4: Perform pharmacokinetic analysis at Duke (Batinic-Haberle and Spasojevic) in rats and mice treated with 0.1 mg/kg BuOE2 SQ. Rodents will be anesthetized and spinal cord, liver, and blood samples will be collected for measurement of BuOE2 at various time points post-injection (4 animals/species / time point). Months 3-12.

This goal was achieved for the mice and is on-going for the rat, with nearly 50% completion. For this experiment, the uninjured rats or mice were given BuOE2 subcutaneously (SC) such that the animal received either one injection (single dose), or a single dose followed 3 days later by ½ the original dose (bi-weekly dose), or a single dose follow 7 days later by ½ the original dose (weekly). At the specified time point, animals were euthanized and the spinal cord, liver, and blood were collected for subsequent assessment of BuOE2 concentration. BuOE2 was extracted from organs and plasma in acetic acid and methanol using a Fast Prep apparatus followed by centrifugation. The levels of BuOE2 in plasma and organs were determined via high-performance liquid chromatography (HPLC) with a tandem mass spectrometer (MS/MS). As seen in figures 1 and 2, we determined that the bi-weekly dosing paradigm induced a significant and sustained tissue level of BuOE2 in the spinal cord.

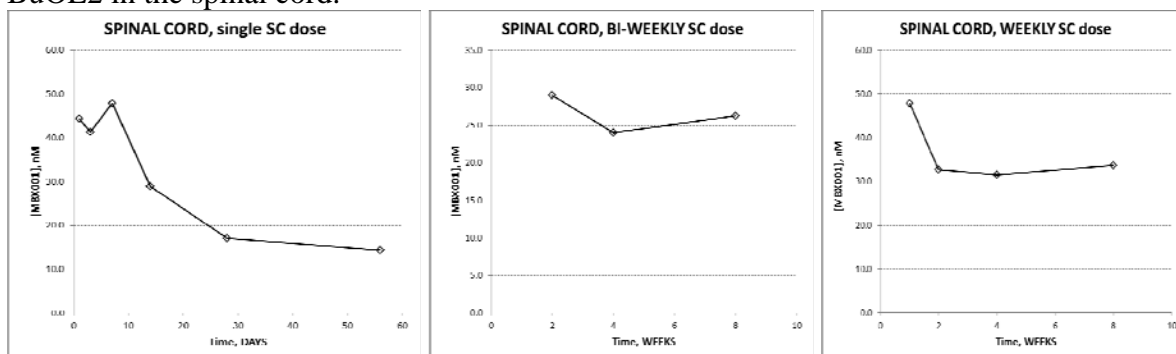Figure 1: Effect of subcutaneous dosing on levels of BuOE2 (a.k.a. MBX001) murine spinal cord. Left panel shows the spinal cord level after a single dose of BuOE2 across several days post-injection. Middle panel shows the effect of a bi-weekly dose of BuOE2 on spinal cord levels measures across several weeks post-injection. Right panel shows the effect of a weekly dose of BuOE2 across several weeks.
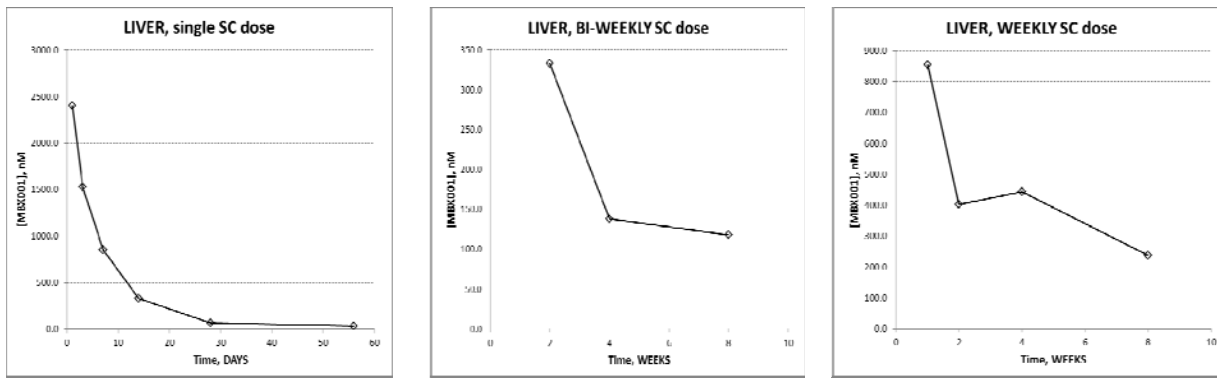
Figure 2: Effect of subcutaneous dosing on levels of BuOE2 (a.k.a. MBX001) murine liver. Left panel shows the spinal cord level after a single dose of BuOE2 across several days post-injection. Middle panel shows the effect of a bi-weekly dose of BuOE2 on spinal cord levels measures across several weeks post-injection. Right panel shows the effect of a weekly dose of BuOE2 across several weeks.

Task 5: For evaluation of ROS, NF-κB, and immunological markers at 24, 72 hr or 7 d post-SCI, induce C5 hemicontusion SCI in 225 male rats at UAB (Floyd) or spinal cord ischemia in 225 male mice at Duke (Warner and Sheng).   Months 3-12.

      a. Sham (all procedures except SCI): n=15
      b. SCI + vehicle: n=15
      c. SCI + 0.03mg/kg/day BuOE2: n=15
      d. SCI + 0.1mg/kg/day BuOE2: n=15
      e. SCI + 0.3mg/kg/day BuOE2: n=15

      This task is ongoing, with nearly 40% completion.   Animals at the 24 hour time point are nearly complete. Assessment at all other time points are on-going, as the PK data was necessary to determine the most effective dosing paradigm. Experiments are underway and we anticipate completion of this task by 2nd quarter next year. As planned, experimental hemicontusion SCI surgery in the rat is being performed at UAB and experimental ischemic SCI in the mice is being performed at Duke. There has been no change from the injury model as described in the original application.   Briefly for induction of SCI in the rat, male Sprague-Dawley rats (250-275g) were anesthetized with inhaled isoflurane and body temperature was maintained at 37C. The mid-cervical vertebral column was exposed and a bilateral laminectomy was performed at vertebral level C5. A moderate (300kdyne) contusion injury was be administered using the Infinite Horizons impactor. For induction of SCI in the mouse, male C57BL/6J mice were anesthetized with isoflurane and placed in the right lateral decubitus position. A left thoracotomy was performed by cauterizing the superficial layer of the intercostal muscle, then inserting the tip of a closed surgical scissor into the thoracic cavity and gently widening the intercostal space by opening the scissor. The thoracic aorta was visualized and a small aneurysm clip was placed on the aorta at the level of T8 to induce ischemic injury. The clip was removed after 10 min.

      We have begun the evaluation of NF-kB signaling at 24 hours post-SCI in the rat. For this experiment, rats were injured and administered BuOE2 after SCI as described above. Spinal cords were extracted at 24h post-SCI, flash frozen, and then homogenized. Tissue was also fractionated using the Active Motif Nuclear Extraction King (catalog #40010) to obtain nuclear fractions. Next, immunoblots were conducted to assess level of total NF-kB (p65, Cell Signaling antibody #8242s) and activated NF-kB (phosphorylated p65, Cell Signaling antibody #3033S). GAPDH (Protein Tech antibody # HRP-6004) was used as a loading control and all protein values as assessed by relative optical density were normalized to GAPDH. Also, each immunoblot included tissue extracts from control (laminectomy only), SCI + vehicle (saline) and SCI + BuOE2 such that

comparisons between experimental groups could be done between samples on the same immunoblot. As seen in figure 3, preliminary data indicate that post-SCI administration of BuOE2 induces a reduction in the level of total NF-kB in the nuclear fraction. With regard to activated NF-kB as detected by phosphorylation at the p65, no difference between injury groups were observed, suggesting that post-SCI BuOE2 may not affect activation of this subunit. Subsequent experiments will follow up on these preliminary findings in both rats and mice.
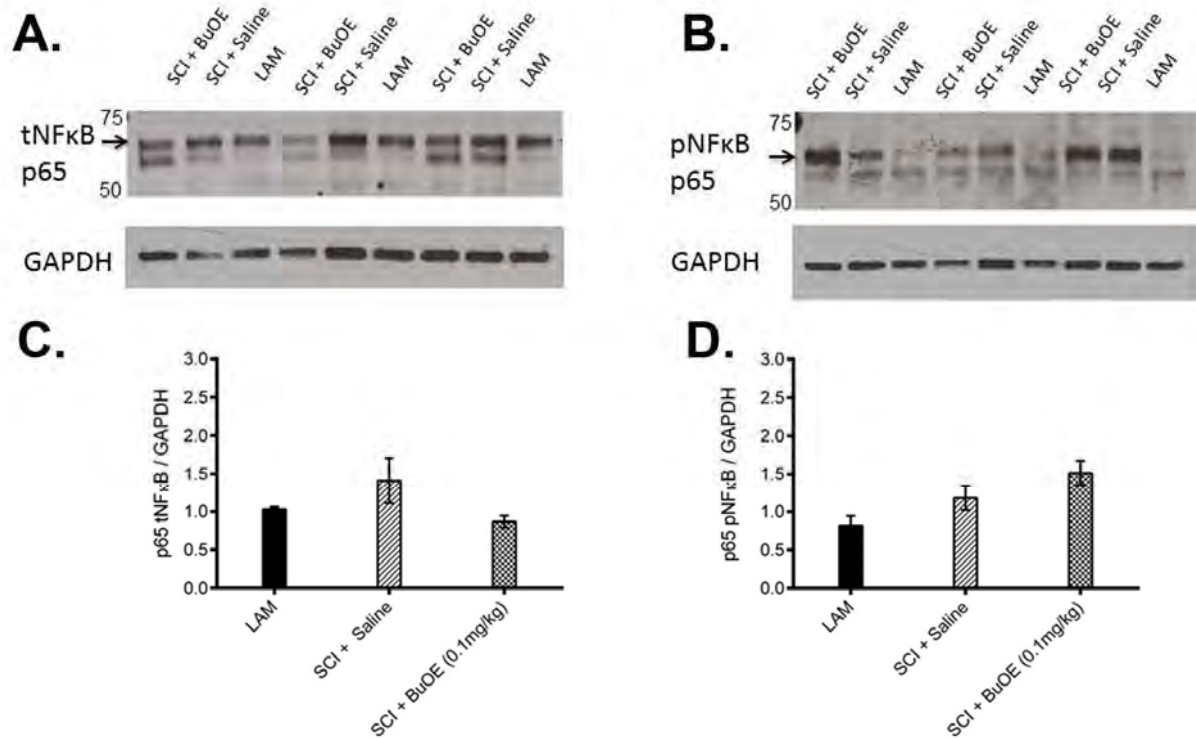

Figure 3: Effect of post-SCI administration of BuOE2 on NF-kB signaling at 24 hours post-injury in the rats. All analyses were conducted at the epicenter of the spinal cord lesion. Panel A is a representative immunoblot probing for total NF-kB (p65) from spinal cord tissue homogenates taken from 9 animals with the group of the animal listed above each lane. GPADH was used as a loading control and the immunoblot corresponding to the lane above is pictured. Panel B is a representative immunoblot probing for phosphorylated (activated) NF-kB (p65) from spinal cord tissue homogenates taken from 9 animals with the group of the animal listed above each lane. GPADH was used as a loading control and the immunoblot corresponding to the lane above is pictured. Panel C is quantification using relative optical density of the total NF-kB protein in the nuclear fraction (from A) protein normalized to GAPDH. Panel D is quantification using relative optical density of the phosphorylated NF-kB protein in the nuclear fraction normalized to GAPDH.

Task 6: At 24, 48 hours, or 7 days post-SCI, exsanguinate a subset of the rats at UAB (Floyd and Tse) or mice at Duke (Warner and Sheng) and rapidly remove and freeze the spinal cord tissue. Next, prepare tissue samples and lysates for subsequent biochemical and molecular analysis and send to Tse lab at UAB (Floyd, Warner, Sheng). Months 3-12.

This task is on-going. Standardized protocols between the collaborative research team have been established and tissue samples have been effectively prepared according to these protocols. The tissue

extraction completion parallels the task 5 completion, and is currently around 40% complete with anticipated completion by 2nd quarter next year.

Task 7: At 24, 48 hours, or 7 days post-SCI, exsanguinate a subset of the rats at UAB (Floyd and Tse) or mice at Duke (Warner and Sheng) and rapidly fix tissue with 4% paraformaldehyde. Remove the spinal cord, cryoprotect, and then block/ freeze the spinal cord segments for subsequent cryosectioning. Collect serial cryosections of the spinal cord for subsequent histochemical and immunohistochemical analysis at UAB and Duke (Floyd, Warner, Sheng). Months 3-12.

This task is on-going. Standardized protocols between the collaborative research team have been established and tissue samples have been effectively prepared according to these protocols. The tissue extraction completion parallels the task 5 completion, and is currently around 40% complete with anticipated completion by 2nd quarter next year.

Task 8: At 24, 48 hours, or 7 days post-SCI, exsanguinate a subset of the rats (Floyd and Tse) or mice (Warner and Sheng) and freeze for subsequent purification of microglia cells and astrocytes from spinal cord tissue by discontinuous percoll gradients or with magnetic beads conjugated to microglia (CD11b)- or astrocyte (GLAST/ACSA-1)-specific antibodies. Conduct flow cytometry experiments from extracted rat or mouse microglia and astrocytes to detect ROS using redox-sensitive dyes and pro-inflammatory cytokines with fluorochrome-conjugated antibodies (Tse). Months 3-12.

This task is on-going. Standardized protocols between the collaborative research team have been established and tissue samples have been effectively prepared according to these protocols. The tissue extraction completion parallels the task 5 completion, and is currently around 40% complete with anticipated completion by 2nd quarter next year.

Task 9: Evaluate pro-inflammatory cytokine/chemokine synthesis in rat or mouse spinal cord protein lysates with a Luminex Beadlyte 21-plex multi-cytokine detection system (Tse). Months 3-12.

This task is on-going, with an estimated completion of 60%. Thus far, we have preliminarily assessed the effect of BuOE2 administration on pro-inflammatory signals tumor necrosis factor alpha (TNFα) and interleukin 6 (IL-6) in the rodent spinal cord at 24 hours post-SCI using enzyme-linked immunosorbent assays (ELISA) for cytokine detection (R&D Systems, TNF alpha DuoSet #DY510; R&D systems IL-6 DuoSet #DY506) . Experimental SCI and post-SCI administration of BuOE2 was induced in the rats and mice as described above. Spinal cord segments from the epicenter and one segment rostral (above the injury level, toward the head) and caudal (below the injury level, toward the tail) of the epicenter were also collected and assessed. Extracted spinal cord was snap frozen and then subsequently homogenized. All values are normalized to protein level and readings are within the standard curves.

Preliminary evaluation of the effect of SCI and post-SCI administration of BuOE2 on TNFα levels at 24 hours post-SCI in the rat is shown in figure 4. We found that SCI induced an increase in the levels of TNFα, particularly in the rostral and caudal segments and that post-SCI administration of BuOE2 reduced levels of TNFα as compared to the SCI+ saline group in tissue at the epicenter. We next evaluated the effect of SCI and post-SCI administration of BuOE2 on IL-6 levels at 24 hours post-SCI in the rat, figure 5. As with TNFα, we found that SCI caused an increase in the levels of Il-6 in the spinal cord (comparisons between LAM and SCI + saline groups). We also observed that levels of Il-6 were reduced in tissue from the group of animals that received BuOE2 post-SCI. With regard to the murine ischemic SCI, we did not find robust differences between groups for the levels of TNFα at 24 hours post-SCI (figure 6). However, when the levels of Il-6 were evaluated in the murine ischemic injury model (figure 7), we found that injury caused an increase Il-6 (comparisons between Sham (lam) and SCI + saline groups)**.** Also, we observed that post-SCI administration of BuOE2

reduced the levels of IL-6, both at the 0.1mg/kg and the 0.3mg/kg group. Additional doses and time points are currently being evaluated to complete this data set and confer a more complete understanding of these effects.
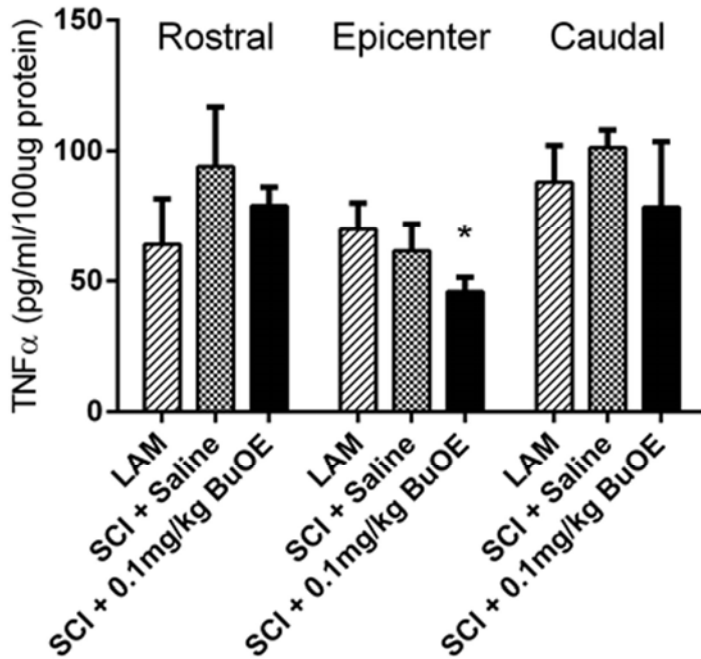
Figure 4: Effect of BuOE2 on expression of TNFα in the rat spinal cord at 24 hours post-SCI. In the rostral and caudal segments, SCI induced an elevation in TNFα as compared to the uninjured control (LAM) that was reduced in the groups administered BuOE2. The reduction in TNFα levels in the BuOE2 group as compared to the SCI + saline group reached statistical significance for tissue at the epicenter of the lesion (*).
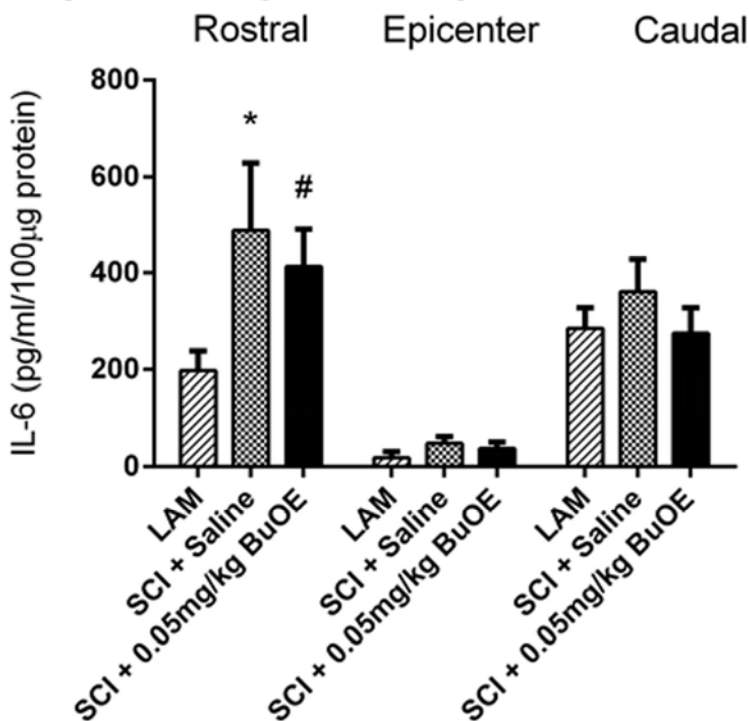
Figure 5: Effect of BuOE2 on expression of Il-6 in the rat spinal cord at 24 hours post-SCI. In the rostral and caudal segments, SCI induced an elevation in Il-6 as compared to the uninjured control (LAM) that reached statistical significant in the rostral segments (*). The levels of Il-6 were reduced in the groups administered BuOE2 as compared to the SCI + saline groups. This reduction reached statistical significance for tissue rostral to the epicenter of the lesion (#).

Mouse SCI - 24h after thoracic aorta clamping
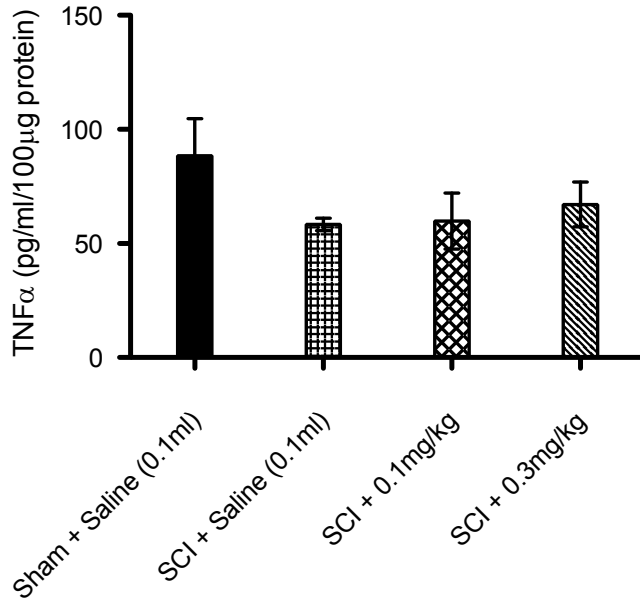
Figure 6: Effect of BuOE2 on expression of TNFα in the murine spinal cord at 24 hours post-SCI. No robust changes in TNFα levels were seen across treatment groups.

Mouse SCI - 24h after thoracic aorta clamping

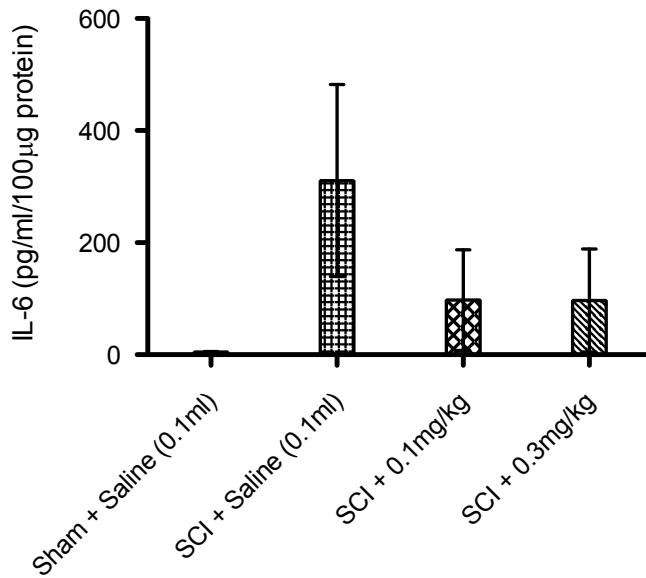Figure 7: Effect of BuOE2 on expression of Il-6 in the murine spinal cord at 24 hours post-SCI. SCI induced an elevation in Il-6 as compared to the uninjured control (sham). The levels of Il-6 were reduced in the groups administered BuOE2 as compared to the SCI + saline groups.

4. IMPACT

      Development of the principal disciplines: The work thus far has had an impact in developing and extending our knowledge on the dose of BuOE2 that results in a steady level in the spinal cord in rodents. Secondly, these studies have begun to examine the effects of post-SCI administration of BuOE2 on inflammation and NF-κB signaling in the spinal cord tissue after contusion and ischemic injury in rodent models.

      Other disciplines: The knowledge concerning the dosing and tissue accumulation of BuOE2 will have an impact on other disciplines in which a therapeutic compound of this type could be used, including but not limited to traumatic brain injury, stroke, alleviation of chemotherapy-induced pain, and diabetic neuropathy.

      Technology transfer: Nothing to report.

      Society: Nothing to report.

5. CHANGES/ PROBLEMS:

Changes in approach:

      1) The data from the TNFα experiment suggest that the 24 hour time point may be too late to observe injury-induced elevations in this important cytokine. It may be important to evaluate this at an earlier post-SCI time point, such as 8 hours. This will be discussed further with the project staff and approval will be received before any changes to the research design are made. These problems do not change the objective or scope of the proposed research.

      2) The data from the NF-κB suggest that phosphorylation of the p65 subunit may not be sensitive to the effects of BuOE2, and thus may not be an optimal readout. We will evaluate other indicators of NF-κB activation including but not limited to assessments at the p50 subunit. This will be discussed further with the project staff and approval will be received before any changes to the research design are made. These problems do not change the objective or scope of the proposed research.

Problems and delays with plan to resolve:

      1) Due to administrative delays, the subcontract agreement between UAB and DUKE University took several months to be signed. This was a one-time delay related to establishing the collaborative agreements in year 1 and this will not occur in subsequent years. We anticipate that the team can accomplish the remaining tasks and objectives from year 1 in the first and second quarter of year 2. To help the team with rapid communication and exchange of data, the PI has set up a goal tracking system using on-line project management software/ data sharing (Basecamp platform). This tracking system will also help the team rapidly exchange ideas to facilitation completion of the remaining tasks from year 1 as well as the year 2 goals.

      Changes with impact on expenditures: Nothing to report.

      Changes in use and care of vertebrate animals: Nothing to report.

6. PRODUCTS

      Submitted Publication:

Comprehensive single and multiple, short and long-term pharmacokinetic studies of redox-active drug and SOD mimic, Mn(III) meso-tetrakis(N-butoxyethylpyridinium-2-yl)porphyrin, MnTnBuOE-2-PyP[5+]

Artak Tovmasyan,[1] Tin Weitner,[1] Huaxin Sheng,[2] Xinghe Chen,[3] Kathleen Ashcraft,[1] Ping Fan,[4] Dewhirst, M. W.,[1] David S. Warner,[2] Zeljko Vujaskovic,[4] Ines Batinic-Haberle[1] and Ivan Spasojevic,[6]*

Departments of Radiation Oncology,[1] Anesthesiology,[2] Medicine,[6] and Duke Cancer Institute,[4] Duke University School of Medicine, Durham, NC 27710, Department of Neurosurgery, The First Hospital of Qinhuangdao City, Hebei, 066000 China,[3] and Division of Translational Radiation Sciences, Department of Radiation Oncology, University of Maryland, Baltimore, Maryland[5]

7. PARTICIPANTS & OTHER COLLABORATING ORGANIZATIONS

NAME	CANDACE FLOYD
PROJECT ROLE	PI
NEAREST PERSON MONTH WORKED	1.2
CONTRIBUTION	Project management, assessment of SCI in rodents
OTHER FUNDING SUPPORT	NIH, UAB, other DoD

NAME	HUBERT TSE, PH.D.
PROJECT ROLE	Co-PI
NEAREST PERSON MONTH WORKED	1.2
CONTRIBUTION	Assessment of cytokines and inflammation, data interpretation
OTHER FUNDING SUPPORT	NIH, UAB, American Diabetes Association

NAME	DAVID WARNER, M.D.
PROJECT ROLE	Co-PI
NEAREST PERSON MONTH WORKED	2.1
CONTRIBUTION	Subcontract project management and oversee the mouse SCI induction
OTHER FUNDING SUPPORT	DUKE

NAME	IVAN SPASOJEVICK, PH.D.
PROJECT ROLE	CO-I
NEAREST PERSON MONTH WORKED	1.2
CONTRIBUTION	Conduct and coordinating the pharmacokinetic assessments
OTHER FUNDING SUPPORT	DUKE

NAME	INES BATINIC-HABER, PH.D
PROJECT ROLE	CO-I
NEAREST PERSON MONTH WORKED	0.9
CONTRIBUTION	assess the purity of BuOE2, assist with data interpretation and PK
OTHER FUNDING SUPPORT	DUKE

NAME	XUZXIN SHENG, M.D.
PROJECT ROLE	3.0
NEAREST PERSON MONTH WORKED	CO-I
CONTRIBUTION	Assessment of ischemic SCI in mice
FUNDING SUPPORT	DUKE

NAME	LONNIE SCHNEIDER
PROJECT ROLE	TECHNICAL (POST-DOC)

NEAREST PERSON MONTH WORKED	12
CONTRIBUTION	Conduct experiments related to rat SCI
FUNDING SUPPORT	NONE

NAME	GARY MASSEY
PROJECT ROLE	TECHNICAL
NEAREST PERSON MONTH WORKED	1.2
CONTRIBUTION	Assist with induction and evaluation of SCI in mice
FUNDING SUPPORT	DUKE

NAME	ARTAK TOVMASYAN
PROJECT ROLE	TECHNICAL (POST-DOC)
NEAREST PERSON MONTH WORKED	1.8
CONTRIBUTION	Assist with PK evaluations
FUNDING SUPPORT	DUKE

8. QUAD CHART

SEE NEXT PAGE

9. APPENDIX

SEE NEXT PAGES

Treatment of Neuropathic Pain after SCI with a Catalytic Oxidoreductant

Insert Award Number/Log Number Here W81XWH-13-1-0482

PI: Candace L. Floyd, Ph.D.   **Org:** University of Alabama at Birmingham/ Duke University **Award Amount:** $946,493

Study/Product Aim(s)

• The proposed research will test the central hypothesis that **post-SCI administration of the catalytic oxidoreductant BuOE will inhibit neuropathic pain after SCI** with the following aims:

•**Aim 1:** Test the hypothesis that post-SCI administration of BuOE decreases ROS, NF-kB signaling, inflammation, and pain-associated behaviors in a clinically relevant *rat* model of *cervical contusion* SCI.
•**Aim 2:** Test the hypothesis that post-SCI administration of BuOE decreases ROS, NF-kB signaling, inflammation, and pain-associated behaviors in a *mouse* model of *ischemic* SCI.
•**Aim 3:** Test the hypothesis that post-SCI administration of BuOE decreases ROS, NF-kB signaling and inflammation after SCI in a *porcine contusion* model.

Approach

Using clinically relevant rodent models of spinal cord injury, we will evaluate the effect of post-injury administration of BuOE on pain-like behaviors in the acute and sub-acute/chronic time period. We will also evaluate effects on NF-kB-dependent pro-inflammatory markers.

Hypothesis

➢ Post-SCI administration of the catalytic oxidoreductant BuOE will inhibit neuropathic pain after SCI

SCI in rats or mice → BuOE → -Pain-like behaviors / -Histology / -ROS and NF-kB signaling

Accomplishment: All institutional approvals, personnel, and techniques in place for initiation of experiments. Year 1 will focus on acute effects of BuOE after SCI in mouse and rat models.

Timeline and Cost

Activities	CY	13	14	15	16
Obtained institutional approvals, trained personnel, initiate studies		�			
Assess effects for SCI: Acute rodent studies			▮		
Assess effects for SCI: Chronic rodent studies				▬	
Assess effects for SCI: Porcine studies					▬
Estimated Budget: DC + ICD ($K)		Y1:287,096	Y2:328,235	Y3: 263,203	

Goals/Milestones:
CY13 Goal – Obtain regulator approval for project
☑ Obtained IACUC, Occupational Health, and ACURO approvals
CY14 Goals – Assess effects of BuOE in acute post-SCI outcomes
☐Investigate effects in rat cervical contusion SCI: acute
☐Investigate effect in mouse ischemic SCI: acute
CY15 Goal – Assess effects of BuOE in chronic post-SCI outcomes
☐Investigate effects in rat cervical contusion SCI: chronic
☐Investigate effect in mouse ischemic SCI: chronic
CY16 Goal – Assess effects of BuOE in large animal SCI model
☐ Assess effects of BuOE in porcine SCI model
Comments/Challenges/Issues/Concerns
• May need to assess early post-SCI time points for inflammatory markers

Updated: 11-10-2014

Comprehensive single and multiple, short and long-term pharmacokinetic studies of redox-active drug and SOD mimic, Mn(III) *meso*-tetrakis(*N*-butoxyethylpyridinium-2-yl)porphyrin, MnTnBuOE-2-PyP5+

by

Artak Tovmasyan,[1] Tin Weitner,[1] Huaxin Sheng,[2] Xinghe Chen,[3] Kathleen Ashcraft,[1] Ping Fan,[4] Dewhirst, M. W.,[1] David S. Warner,[2] Zeljko Vujaskovic,[4] Ines Batinic-Haberle[1] and Ivan Spasojevic,[6]*

Departments of Radiation Oncology,[1] Anesthesiology,[2] Medicine,[6] and Duke Cancer Institute,[4] Duke University School of Medicine, Durham, NC 27710, Department of Neurosurgery, The First Hospital of Qinhuangdao City, Hebei, 066000 China,[3] and Division of Translational Radiation Sciences, Department of Radiation Oncology, University of Maryland, Baltimore, Maryland[5]

*Corresponding author

Ivan Spasojevic, PhD
Department of Medicine
PK/PD Duke Cancer Institute Shared Resource
Duke University School of Medicine, Durham, NC 27710
Tel: 919-684-8311
e-mail: ivan.spasojevic@duke.edu

Abstract

Cationic Mn(III) *N*-substituted pyridylporphyrins (MnP) have been optimized to increase their biodistribution and toxicity without compromising their redox-active properties. Most recent analog, MnTnBuOE-2-PyP^{5+}, has been synthesized and its therapeutic effects assessed. It possesses a high ability to catalyze O_2^- dismutation (SOD-like activity) and peroxynitrite ($ONOO^-$) and hypochlorite ($HClO^-$) reduction, and impact cellular metabolism at least in part affecting cellular transcription activity. Its distribution and efficacies in central nervous system injuries and in mitochondria have been well-documented. Along with efficacy studies comprehensive pharmacokinetic (PK) studies were conducted to evidence its biodistribution and facilitate the proper dosing regime and identify preferred routes of administration. A single 72 h-PK mouse study was performed *via iv* and *sc* routes; the levels in plasma, liver, kidney, spleen, colon, heart, lung and brain were determined and PK parameters, AUC, $t_{1/2}$, C_{max} and t_{max} calculated. Highest levels were found in liver and kidney, followed by lung, heart and spleen, while the lower levels were demonstrated in colon and the lowest in brain. Further, a long-term 56-day single and multiple dosing PK study *via sc* route at 4 different concentrations of 0.5/kg, 1 mg/kg, 3 mg/g and 10 mg/kg, was conducted. MnP was given as **(i)** a single injection, **(ii)** once weekly and **(iii)** once every second week. The levels of MnP in liver, brain, spinal cord, salivary glands, and tongue were measured and PK parameters, AUC, $t_{1/2}$, C_{max} and t_{max} calculated. Finally, accumulation of MnP at one day, 7 and 28 days of twice-daily administration of 4 doses (0.5, 1.5, 4.5 and 9 mg/kg) was conducted. No saturation levels were reached at 28 days of such dosing. No change in mouse weight was observed at any dose. The accumulation of MnP in brain and spinal cord is slower than in other organs where the pharmacokinetics follows the liver profile. The oral availability of three lead MnPs, MnTE-2-PyP^{5+}, MnTnHex-2-PyP^{5+} and MnTnBuOE-2-PyP^{5+}, was re-evaluated to be 0.6, 2.9 and 3.9%; it follows trend in their hydrophilicities, MnTE-2-PyP^{5+} being the most hydrophilic one. The mouse perfusion, prior to organ extraction has been a routine strategy to avoid the contribution of blood MnP levels in organ measurements. We have demonstrated herein that such approach is safe as it does not extract MnP from the tissue.

Introduction

MnTnBuOE-2-PyP^{5+} is an optimized cationic, fairly lipophilic Mn(III) *N*-butoxyethylpyridylporphyrin with favorable interplay of redox activities bioavailability and lipophilicity. Its redox properties are accurately described by its metal-centered reduction potential for Mn^{II}P/Mn^{II}P redox couple and ability to catalyze O_2^- dismutation, log $k_{cat}(O_2^-)$]. It crosses blood brain barrier and accumulates in both brain and heart mitochondria [1, 2]. It is few fold less toxic than otherwise similarly lipophilic analog, MnTnHex-2-PyP^{5+} [3, 4]. Differences in the structure of pyridyl substituents between these two Mn porphyrins are not yet fully understood, but affect their bioavailibilities [3, 4]. Both compounds have 6 C atoms in their pyridyl substituents. Yet, MnTnBuOE-2-PyP^{5+} has one oxygen atom in each of four pyridyl substituents; subsequently it is slightly more hydrophilic that MnTnHex-2-PyP^{5+}. Its polar oxygen atoms with 2 electron pairs, each, seemingly affect its transport into mitochondria and retention in lipid membranes, brain included [1, 2].

Both compounds are under preclinical exploration *in vitro* and *in vivo*. MnTnBuOE-2-PyP[5+] has been firstly tested in an O_2^- specific *in vivo* model – aerobic growth of SOD-deficient yeast *Saccharomyces cerevisiae* where it allows this organism to grow as well as wild type [4, 5]. It has then been forwarded into other cellular and animal models as well as biodistribution studies. MnTnBuOE-2-PyP[5+] was shown to accumulate in brain and its parts [1-3, 6] and in brain and heart mitochondria [1, 2, 7]. The direct evidence was provided that MnTnBuOE-2-PyP[5+] mimics mitochondrial SOD isoform, MnSOD. The work was done on MnSOD over-expressor- and knock-out mice, where MnTnBuOE-2-PyP[5+] protects HaCaT human keratinocytes against UV radiation-induced oncogenic transformation *via* inside-out signaling [8]. MnTnBuOE-2-PyP[5+] also suppresses doxorubicin-induced mitochondrial dysfunction in neonatal rat heart cells H9C2 [8, 9] [Miriyala et al., submitted]. In a mouse model this MnP affords whole brain radioprotection [10, 11]. MnTnBuOE-2-PyP[5+] [10]10 and MnTnHex-2-PyP[5+] [3] acted as radio- and chemo-sensitizors in a D-245 MG glioblastoma sc mouse xenograft model. Further, in a mouse head and neck radioprotection model MnTnBuOE-2-PyP[5+] protects salivary glands [12], while in a head and neck tumor sc xenograft mouse study MnTnBuOE-2-PyP[5+] acted as radiosensitizer suppressing tumor growth [12]. In such scenario, MnP employs H_2O_2 to catalyze thiol oxidation of numerous proteins which results in tumor cell death [13-16]. The differential actions of MnP with respect to tumor (cytotoxic) and normal tissue (radioprotective), arising from their different redox environment, make MnPs prospective candidates as tumor radio- and chemo-therapeutics. Recently, instead of radiation, the MnP/ascorbate system was used as a ROS generator and promoted tumor death in cellular and animal studies [3, 17-19]. In a cellular lymphoma model, MnTnBuO-2-PyP[5+] and MnTE-2-PyP[5+] enhanced the anticancer effect of dexamethasone (Tome et al, unpublished) [13, 14]. Erectile dysfunction is a serious side effect of prostate radiation and greatly reduces willingness of patients to undergo such treatment. In a rat prostate radiation model, MnTnBuOE-2-PyP[5+] was able to greatly rescue erectile function in a similar fashion to the action of its analog, MnTE-2-PyP ([20], Oberley et al unpublished). We have further shown the potency of MnTnBuoE-2-PyP[5+] in suppressing chronic morphine tolerance in a mouse model under conditions previously reported for earlier analogs MnTE(or nHex)-2-PyP[5+] ([21] [Warner et al, unpublished]. MnTnBuOE-2-PyP[5+] exhibited remarkable ability to minimize itch in a mouse model [22] [Ji, Liu et al, unpublished]. Itch was induced *via* chloroquinone, which activates pruriceptors or compound 48/48. Compound 48/48, which promotes histamine release, is a polymer produced by the condensation of *N*-methyl-*p*-methoxyphenethylamine. MnTnBuOE-2-PyP[5+] increased survival and reduced long-term movement deficit in a galactose-1P uridylyltransferase-null mouse model of galactosemia [23]. Thus far, MnTnBuOE-2-PyP[5+] was tested in mice and rats at single and multiple dosing in the range of 0.1 to 3.2 mg/kg per day given daily or several times per week for up to 6 weeks *via* ip or *sc* routes. In cellular studies it was efficacious in a range of 0.1 to 20 μM, depending upon the type of a cell. **Figure 1** summarizes the *in vitro* and *in vivo* therapeutic effects of MnTnBuOE-2-PyP[5+] [1-12, 15].
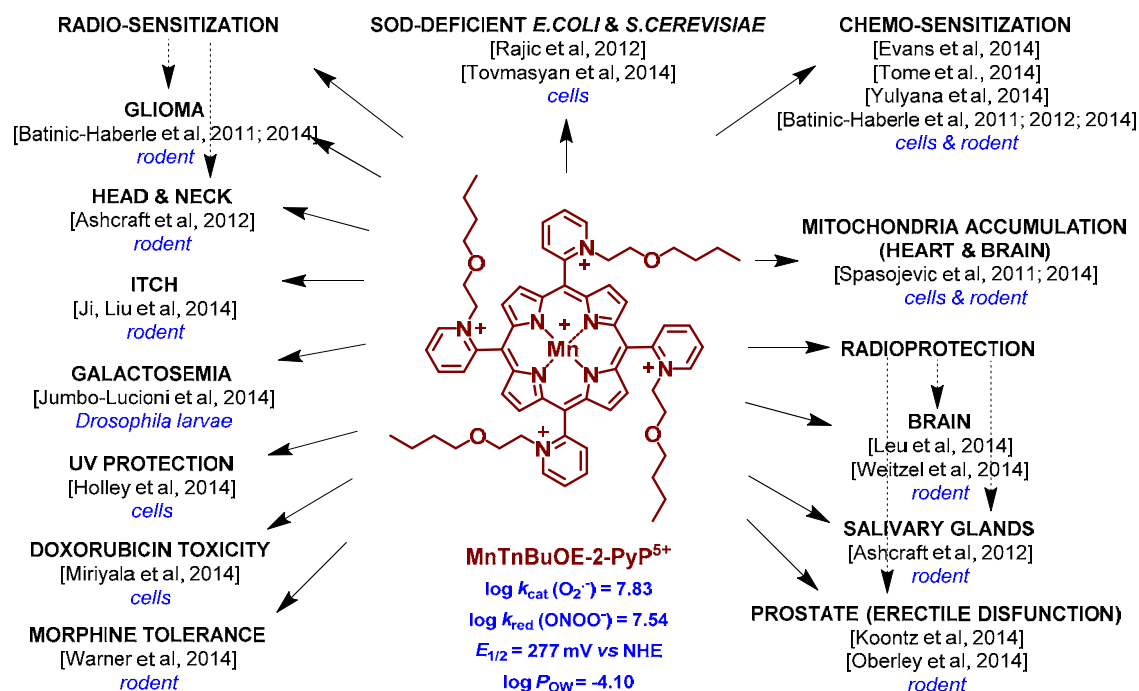
Figure 1. The *in vitro* and *in vivo* therapeutic effects of MnTnBuOE-2-PyP^{5+} (BMX-001). Also listed are: metal-centered reduction potential for Mn^{II}P/Mn^{III}P redox couple, $E_{1/2}$, the ability of MnP to catalyze O_2^- dismutation, log $k_{cat}O_2^-$, the ability to reduce ONOO$^-$ and lipophilicity in terms of partition between n-octanol and water, log P_{OW}.

Artak, add subarachnoid hemorrhage as unpublished, add mucose at salivary glands" Salivary Glands & Mucose

The initial therapeutic effects observed have justified the subsequent comprehensive PK studies. We have herein determined the maximal tolerable single dose *via iv* and *sc* routes of administration. Subsequently we performed a single PK study *via sc* and *iv* routes and analyzed MnP in all major organs: liver, kidney, spleen, lung, heart, brain, spinal cord and colon. To account for the preclinical studies targeting brain and head and neck cancer and radioprotection we have assessed levels in brain, salivary glands and tongue also. Due to our interest in developing Mn porphyrins for the injuries of central nervous system, spinal cord was analyzed also. The 24-hour single injection PK study was followed with a long-term comprehensive 56-day multiple dosing PK study at 4 different concentrations. The goal was to provide the information on the frequency of dosing needed to maintain levels in organs high enough to assure therapeutic efficacy, *i.e.* avoid toxic.

The reports on PK studies of Mn porphyrins and drugs in general are rare, while essential for proper therapeutic effects [24] Moreover, usually only plasma PK profiles are reported, and very rarely organ levels (see references in [24].

Experimental

Porphyrins and other chemicals. MnTnBuOE-2-PyP^{5+} (λ_{max} = 454.0 nm, log ε = 5.14), and MnTnHep-2-PyP^{5+} (λ_{max} = 454.0 nm, log ε = 5.19) as a standard were synthesized and characterized as previously described [25, 26]. Other chemicals used were acetonitrile (MeCN) by Fisher Scientific, methanol (anhydrous, absolute) by Mallinckrodt, glacial acetic acid by EM Science, heptafluorobutyric acid (HFBA) by Aldrich and phosphate-buffered saline (50 mM sodium phosphate, 0.9% NaCl, pH7.4) by Gibco.

Mice. Duke University Medical Center Animal Facility has a continuously accredited program from AAALAC International. All experiments using animals were performed according to the approved protocol for humane care and use of animals. The 10-weeks old C57BL/6J female mice weighing 17-25 g were used.

Maximal tolerable dose. Firstly, the maximal tolerable dose was determined for *sc* and *iv* route by step-wise increasing the dosing with 3 mice per dose until significant impact on mouse behavior, such as quietness, reluctance to move some of those caused by acute blood pressure drop, was observed. A single *sc* dose of 10 mg/kg of MnTnBuOE-2-PyP^{5+} and *iv* dose of 2 mg/kg were identified as MTD. The concentration of aqueous solutions (for oral gavage) or saline solutions (for subcutaneous, sc and intravenous, iv injections) of MnTnBuOE2-PyP^{5+} was adjusted so that mice were injected with ~ 0.1 mL per dose.

Single dose 72h-PK study. In a single dose 72-h Pk study the *sc* and *iv* dosing were compared, the plasma and organ levels were analyzed at different time points within 72 h. For *iv* injections mice were anesthetized with isoflurane in 30% oxygen balanced with nitrogen and a PE-10 tubing was surgically implanted into right jugular vein. 0.1 ml BuOE2 solution was slowly infused using 1 ml syringe. Then the PE-10 tubing was removed and skin incision was closed. Mouse was returned into the cage after injection. For PK studies, mice were euthanized at different time points (5 min to 24 hours), with 3 mice per time point.

Long-term 56-day single and multiple dosing sc PK study. This study was conducted at 4 different doses of 0.5, 1, 3 and 10 m/kg, given *via sc* route. Analyses were done for: **(i)** single dosing at days 1, 3, 7, 14, 28 and 56 days; **(ii)** weekly dosing at 7, 14, 28, and 56 days; and **(iii)** every second week at 14, 28, and 56 days.

Long-term 7-day and 28-day PK study. MnTnBuOE-2-PyP^{5+} was given *sc* in two daily increments at 4 different doses of 0.5, 1.5, 4.5 and 9 mg/kg given for the duration of 1 day, 7 days and 28 days. Samples were taken as described below for tissue collection at 12 hours after the last injection. 13 groups of mice (including control group with no drug administration) with 3 mice per group were analyzed. 3 mice per group were analyzed.

Organ collection. In all studies mice were perfused prior to tissue collection. Exception was only a study where comparing perfusion vs non-perfusion method used in tissue collection was compared. The perfusion was conducted in following way. Mice were re-anesthetized with 5% isoflurane in 30% oxygen balanced with nitrogen. Then mice were intubated and mechanically controlled by a rodent ventilator (Harvard model 683) with the tidal volume of 0.7 ml and the rate of 105 strokes/minute. Isoflurane was reduced to 1.8% for subsequent procedure. The chest was open to explore the heart. 0.5 ml arterial blood was directly sampled from left ventricle. Then a blunt 20 gauge needle was inserted into aorta via left ventricle and a small cut was made on right atrium. The vasculature was

briefly rinsed with 60 mL saline by transcardial perfusion prior to excision of liver, kidney, spleen, lung, heart, and brain. Fresh blood mixed with heparin was centrifuged at 2500 rpm for 10 minutes. Plasma and hematocytes were separated immediately. Samples were kept at -80^0C.

MnP extraction from plasma and organs. Organs were cryo-pulverized in a Bessman tissue pulverizer (BioSpec Products, Bartlesville, OK) under liquid nitrogen and then homogenized in a rotary homogenizer (PTFE pestle and glass tube) with 2 volumes of deionized water. An aliquot of either plasma or tissue homogenate was transferred into a 2 mL polypropylene screw-cap vial and a double volume of 1% acetic acid in methanol was added and mixed by vortexing for 30 sec (1:2 homogenate:1% acetic acid). Samples were treated twice in the FastPrep apparatus (Qbiogene, Carlsbad, CA) at speed 6.5 for 20 sec and subsequently centrifuged 10 min at 13,000 g to separate proteins. An aliquot of the supernatant was pipetted into a 5 mL polypropylene tube (10×50 mm) and the solvent was completely removed in a Savant Speed-Vac evaporator at 40^oC within 1 h. The dry residue was dissolved in a 20 μL of mobile phase B (see below) and sonicated for 5 min, then 80 μL of mobile phase B was added, the mixture was sonicated again for 5 min and centrifuged for 5 min at 4500 g at 4^oC. Finally, the tube content was transferred to the HPLC autosampler polypropylene vial equipped with silicone/PTFE septum, followed by another cycle of centrifugation for 5 min at 4500 g (4^oC), after which the sample was immediately analyzed by LC-MS/MS.

LC-MS/MS analysis of MnP levels in plasma and organs. Quantitative analysis was performed on a Shimadzu 20A series HPLC (LC) - Applied Biosystems MDS Sciex 3200 QTrap or 4000 QTrap tandem-mass spectrometer (MS/MS) at Pharmacology Laboratory (Shared Resource PK/PD and Small Molecule Analysis Core) of Duke Cancer Center. The use of HFBA as an ion-pairing agent increases overall lipophilicity/volatility and greatly improves retention and ionization efficiency of the analytes, affording an abundance of $[MnP^{5+} + 2HFBA^-]^{3+}$ and $[MnP^{5+} + 3HFBA^-]^{2+}$ ions. Solvents employed were: A = 95:5 H_2O:MeCN (0.1% HFBA); B = MeCN (0.1% HFBA). MnTnBuOE-2-PyP^{5+}, like all *ortho* Mn(III) *N*-substituted pyridylporphyrins, exists as a mixture of four atropoisomers. With the chosen solvent system all four atropoisomers of MnPs [27] collapsed into a single peak enhancing the sensitivity of the method to as low as 0.5 nM (nanomoles per mL of tissue homogenate). Analyses were performed using a Phenomenex Luna C18 guard cartridge (ID x L, 2 x 4 mm) only. Specific mass transitions m/z $[MnP^{5+} + 3HFBA^-]^{2+}$ to m/z $[MnP^{5+} - alkyl^+]$ fragmentation were followed: MnTnBuOE-2-PyP^{5+} at m/z = 857.3/599. For short 24-h PK study MnTnHep-2-PyP^{5+} was used as internal standard at m/z 853.5/639.5. For long term 56 day PK multi-dosing PK study, the deuterated, MnTnBuOE-2-PyP^{5+}-d_8 compound was used as internal standard with m/z = 862.2/603.9. Deuterated compound was obtained from Albany Molecular Research who GMP-scaled up the compound. Calibration samples in 1–300 nM or 0.1–30 μM range (depending on the expected levels of MnP) were prepared by adding known amounts of serially diluted pure standards into homogenates of the corresponding tissues and were analyzed along with study samples. Response was calculated as the ratio between the standard peak area and internal standard peak area. The extraction of a lipophilic MnTnBuOE-2-PyP^{5+} and the preparation of the plasma and tissue samples for analysis has been further improved in this study. Relative to

hydrophilic MnTE-2-PyP^{5+}, the analysis of lipophilic MnPs is more challenging due to their affinity for proteins and plastic and glass surfaces. Thus, each MnP needs specific method adjustments as well as different internal standard.

Re-evaluation of oral availability. We have reported that cationic Mn(III) *N*-alkylpyridylporphyrins (MnTE(or nHex)-2-PyP^{5+}) are ~ 20% orally available [24]. We have subsequently performed, in a same manner as with MnTE(or nHex)-2-PyP^{5+}, a single-dose 72-h oral availability PK study for alkoxyalkyl analog, MnTnBuOE-2-PyP^{5+} [1-3, 24, 28]. When we subsequently tried to assess the outcome of a long-term oral administration of MnTnBuOE-2-PyP^{5+} *via* drinking water, no significant MnP levels in plasma and liver were found; no aversion of mice to drinking was observed as expected daily amount of water per mouse was consumed. Another long-term comprehensive study with MnTnHex-2-PyP^{5+} followed. Doses as high as 2 and 5 mg/kg/day were given *via* oral gavage. MnTnHex-2-PyP^{5+} was given daily for **(i)** one week; **(ii)** two weeks; **(iii)** three weeks, and **(iv)** 4 weeks. MnP levels in liver were determined with all 4 dosing regims at **(a)** 2 hours; **(b)** 6 hours, and **(c)** 24 hours post last oral gavage. When 5 mg/kg MnP was given for a week, the liver levels at 24 hours after oral gavage (where no contribution of plasma levels to MnP organ levels were expected as mice were perfused) were low, ~ 36 to 78 nM; the expected values were projected based on earlier study to be well above 4,454 nM. For the sake of precision in collecting plasma and organs during early time points, we gave drug orally directly into the stomach of anesthetized mouse in a following way. The 7-8 cm blunt polyethylene tubing PE-50 tube was connected to a 1 ml syringe. Tubing was marked 5 cm from the tip to know when it reaches stomach. Mouse was anesthetized in the chamber containing 5% isoflurane in 30% oxygen balanced with nitrogen. The PE 50 tube was gently inserted into esophagus and advanced into stomach along the left wall of mouth. The tube was advanced until the mark on the tube reaches nose of the mouse. The 0.1 ml of compound was infused. Then the tube was slowly withdrawn. It appeared that such strategy might have allowed for a reflux into the respiratory pathways. At alter time points beyond 2 h drug was give into the mouth cavity of awaken mouse.

We were for a while puzzled with large scattering of the data within early time period of a PK profile for all three MnPs, MnTE(or nHex or nBuOE)-2-PyP^{5+} [24]. We had initially attributed such scattering to the differences in the oral absorption among individual mice. Yet, it was not before we failed to detect MnP in a liver in a long-term oral gavage study, that we reconsidered the scattering of the data within early time points. The only difference between the early and later time points was in the way how we administered drug orally: into the stomach *vs* mouth cavity. We believed that our strategy of giving drug directly into the stomach of anesthetized mouse was a precise approach in collecting blood and organs at very early time points. Reflux was not anticipated as it was commonly assumed that any entrance of a drug into respiratory system would cause huge distress or even death of a mouse. While anesthetized during drug delivery, mice were in horizontal position supplied with artificial breathing. *All 3 conditions combined - anesthesia, horizontal position and artificial breathing - allowed for the reflux of a drug into the respiratory system and subsequently into the plasma and accounted for ~20% of intravenous levels.*

To prove such hypothesis, we designed a study depicted in **Table 1**. In addition to traditional oral gavage into the mouth cavity, we administered MnTnHex-2-PyP^{5+} directly into the respiratory system, at 20% and 10% of the total 2 mg/kg dose given into the mouth or stomach. We kept the mouse anesthetized either with or without artificial breathing through 2 h-duration of the study. We also had a group of mice where no anesthesia was applied

(groups 3 and 6). We also have a group of mice where we injected drug directly into intestine to account for possible intestine availability only. In another group of mice, we sutured the stomach to prevent MnP availability *via* intestine. MnP reaches C_{max} in plasma very fast, for *sc* route it was found to be ~ 1hour. Thus, the plasma MnP levels were determined at 10 min and 2 hours. No significant absorption of MnP *via* stomach or intestine was demonstrated. The 100% of a drug given into oral cavity of non-anesthetized mouse without artificial breathing does not reach plasma at any significant level. Artificial breathing greatly enhanced reflux: 20% of 2 mg/kg given into the mouth of anesthetized mouse with artificial breathing reaches blood at significantly higher levels (**Figure 1**). When 10% of the total drug was given into trachea of a mouse under artificial breathing the amount found in plasma of ~113 nM at 10 min post-injection was 5-fold higher than when 100% of a dose was given into the mouth of awaken mouth (24 nM) (compare groups 3 and 6 in **Figure 1**). The 113 nM levels which presents the 10% availability of 2 mg/kg dose *via* trachea agree well with data we reported on oral availability achieved within first minutes post administration reported [24]. The assumption is here made that the whole amount of MnP which enters trachea reaches the blood. We then recalculated the oral availability accounting for the period 2 h to 24 h only when the drug was given *via* oral gavage into the mouth (**Figure 2**). It was found to be 2.9% (**Figure 2**). The oral availability of MnTnBuOE-2-PyP^{5+} was initially calculated in the same way as MnTnHex-2-PyP^{5+} and with MnTE-2-PyP^{5+} to be ~20% [3, 24] (**Figure 2B**). It was then recalculated here to be 3.9% (**Figure 2A&C**). The 0.6% oral availability of MnTE-2-PyP^{5+} was recalculated in the same way (**Figure 2A&C**) in agreement with more hydrophilic nature of this porphyrin. Our re-assessment of the oral availability of cationic Mn porphyrins agree with the outcome of efficacy study published by Salvemini's group where the lack of the protective effect of MnTE-2-PyP^{5+} in carrageenan-induced hyperalgesia was demonstrated when it was given *orally*, but not *ip* [29].

Table 1. Re-evaluation of the MnP oral availability. The study was designed to provide evidence that the drug reflux into respiratory system during oral gavage experiment accounted for high blood and organ oral availability. MnTnHex-2-PyP^{5+} was given to anesthetized mouse with and without artificial breathing, and was analyzed in plasma at 10 min (shown below) and 2 hours. Different ways of administration were herein explored to differentiate the drug access to blood: *via* oral GI tracts or *via* respiratory system.

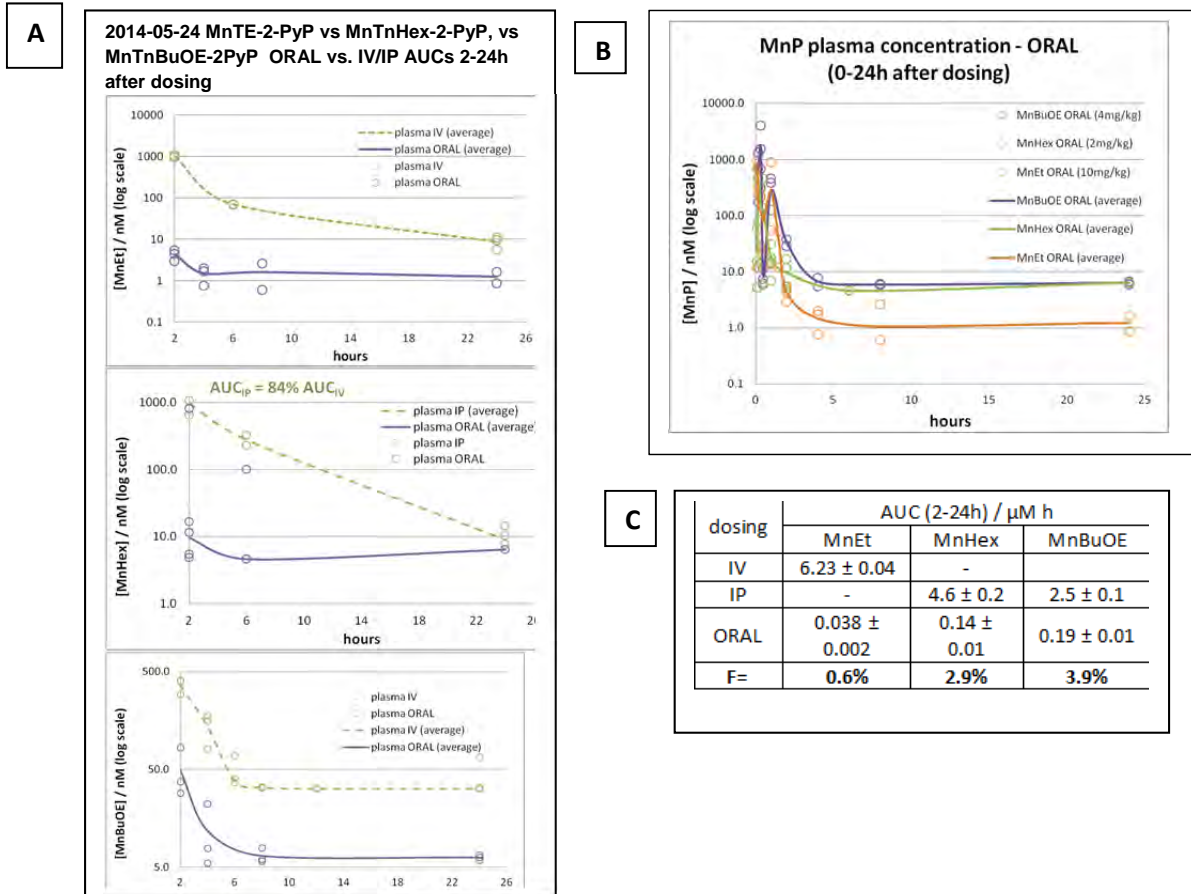| Group	Delivered	Inhalation Anesthesia (isoflurane)	Comments
1	Intestine (100% dose)	yes	Sutured towards stomach
2	Stomach (100% dose)	yes	Sutured towards intestines and esophagus
3	Oral cavity (100% dose)	no	With a OG needle (slow delivery)
4	Oral cavity (20% dose)	yes	20 uL
5	Trachea (10% dose)	yes	By PE10 tubing
6	Trachea (10% dose)	no	By PE10 tubing
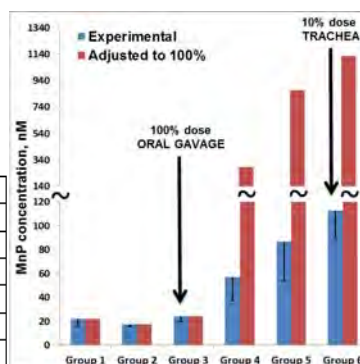
Figure 2. The re-evaluation of the oral availability of lipophilic Mn porphyrins, MnTE-2-PyP^{5+}, MnTnHex-2-PyP^{5+} and MnTnBuOE-2-PyP^{5+}. (A) PK profiles of all 3 Mn porphyrins when given into the mouse cavity *via* oral gavage for a period of 2-24 h; **(B)** The PK profiles for all 3 MnPs for the period of 0-24 h. During early time points MnP was given *via* polyethylene tubing into the stomach. As mouse was anesthetized and supplied *via* artificial breathing, some of the drug entered respiratory system and in turn blood and artificially increased blood MnP levels. **(C)** Recalculated data accounting only for 2-24 h period of time when MnP was given into mouth cavity of awaken mouse and when no significant scattering of data was observed [24]. The 2.9% of oral availability was obtained for MnTnHex-2-PyP^{5+} which agrees well with the study conducted herein and laid out in **Table 1**. The similar, 3.9% oral availability was obtained for MnTnBuOE-2-PyP^{5+}. As anticipated, few fold lower oral availability of 0.6% of MnTE-2-PyP^{5+} was obtained for the most hydrophilic compound among three MnPs studied.

Evaluation of the perfusion vs non-perfusion strategy in extracting plasma and organs while assessing MnP PK profile.

Herein we analyzed the mice liver MnTnHex-2-PyP^{5+} levels at 7 days after 10 mg/kg sc injection. 12 mice were distributed in 3 groups, 4 mice per group: **(i)** non-perfused; **(ii)** perfused either 30 mL; **(iii)** perfused with 60 mL saline. Perfusion was performed as described under MnP plasma/tissue extraction. The data are relevant to MnTnBuOE-2-PyP^{5+} which has similar biodistribution. In all 3 groups of mice the levels found in plasma at 7 days after 10 mg/kg sc injections were essentially identical.
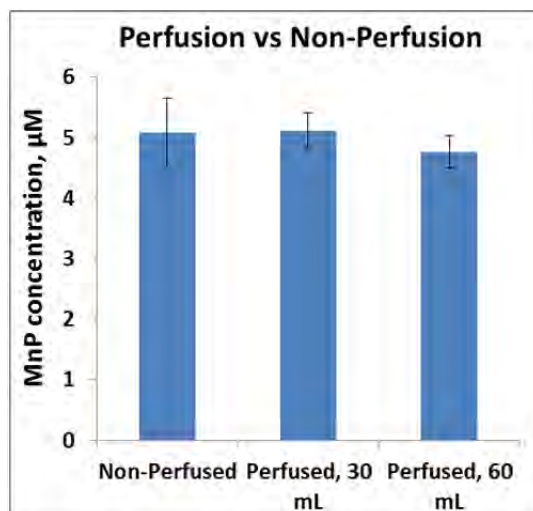
Figure 3. Evaluation of the impact of mouse perfusion prior to organ collection on the organ levels of MnTnHex-2-PyP^{5+}. The livers of mice were analyzed at 7 days after *sc* 10 mg/kg single injection. 4 mice were analyzed per group. The data show that perfusion with 30 mL or 60 mL of saline did not reduce levels of MnP in organs.

Results and Discussion

The pharmacokinetic profiles are essential for the proper dosing of a drug in order to achieve the maximal therapeutic efficacy. Therefore single *sc* and *iv* 24-hour, and multiple long-term single injection, daily, weekly, and every second week, over 28 and 56 days (8 weeks), at 4 different doses PK studies were conducted to account for the biodistribution and clearances of MnP from target organs when drug was given for a long period of time.

Single dose 7-day sc and iv pharmacokinetic study. The single dose PK study was conducted with 10 mg/kg *sc* and 2 mg/kg *iv* injections identified as MTD. The PK curves are shown for several major organs in **Figure 4.** All data are provided in *Supplemental Material,* Figure 1S.
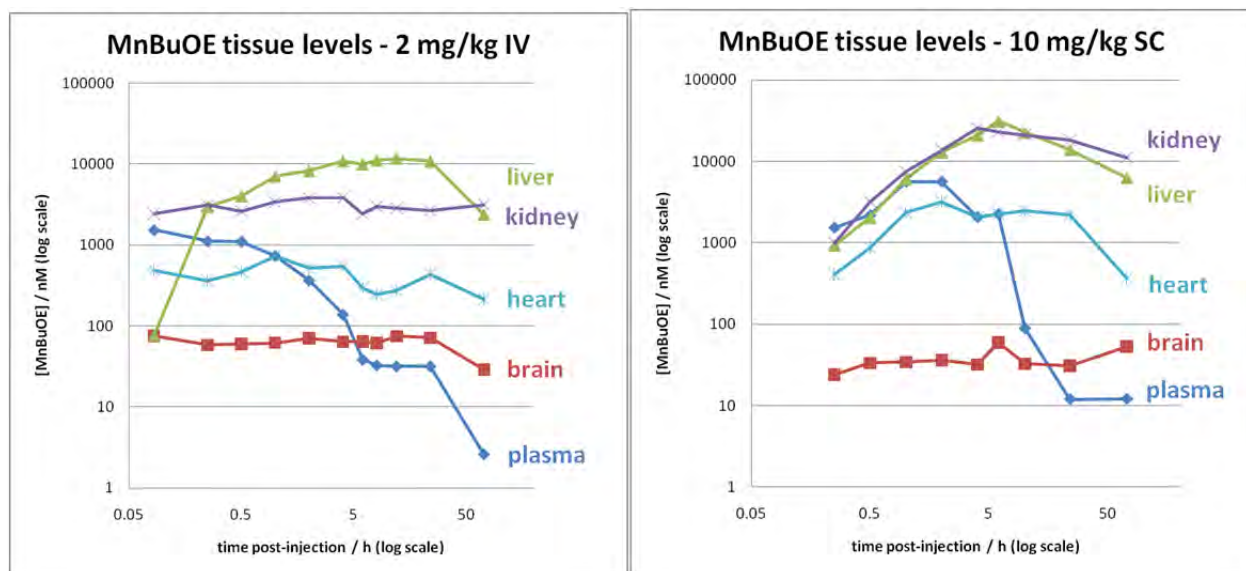
Figure 4. The 72-hour single dose plasma and organ *sc* and *iv* PK profiles of MnTnBuOE-2-PyP^{5+}. MnTnBuOE-2-PyP^{5+} was given *sc* at 10 mg/kg or *iv* at 2 mg/kg. The levels are given in nanomoles per 1000 mL of plasma or tissue homogenates. Time post-injection on x-axis is presented in log scale.

Non-compartmental analysis (WinNonlin; Pharsight, Inc.) was used to calculate the pharmacokinetic parameters given in **Table 2**. The biodistribution of MnTBuOE-2-PyP^{5+} in organs *via sc* relative to *iv* route of administration was given in **Figure 5**. Plasma drug body exposure was higher with *sc* then with *iv* route due to the higher clearance of MnP from plasma *via iv* route. As our earlier data on MnTE-2-PyP^{5+} and MnTnHex-2-PyP^{5+} show [24, 30, 31], the lowest availibility of this class of compounds was found in brain at 24 hours. Yet the long term 56-day PK study (see below) indicates that the MnP accumulation continues in brain during 10 days. The data In Figure 4 show that as MnP cleares from plasma, it continues to accumulate in all organs. Liver, kidney and spleen seve as reservoirs for the MnP accumulation and maintainance in other organs.

Table 2. **The 72-hour single dose *sc* and *iv* pharmacokinetic parameters of MnTnBuOE-2-PyP^{5+} for plasma and all organs**. MnTnBuOE-2-PyP^{5+} was given *sc* at 10 mg/kg or *iv* at 2 mg/kg. The AUC, C_{max}, t_{max} and clearance, $t_{1/2}$ (where a level decline was observed in the period 24-72 hours), were calculated.

| Parameter→	AUC (µM h)					C_{max} (µM)				t_{max} (h)				$t_{1/2}$ (h)			
Sample ↓	IV	sd	SC	sd	F (%)	IV	sd	SC	sd	IV	sd	SC	sd	IV	sd	SC	sd
plasma	3.40	0.04	23.58	0.33	139	1.5	0.1	6.2	0.3	0.1	0.1	1.3	0.6	31	1	-	-
brain	3.91	0.02	2.82	0.02	14	0.083	0.002	0.06	0.01	4.1	6.9	28.0	38.1	85	8	-	-
liver	520.4	5.1	926.1	9.2	36	13.1	1.2	27.6	6.5	7.3	1.2	5.3	1.2	51	2	97	9
kidney	209.1	1.5	1160.4	14.9	111	4.1	0.4	29.1	2.4	2.0	1.7	5.3	1.2	-	-	158	33
spleen	60.5	0.5	115.8	8.1	38	1.7	0.3	2.2	0.3	13.3	9.2	28.0	38.1	58	4	-	-
lung	20.5	0.6	93.0	1.2	91	1.3	0.2	6.6	0.5	0.9	0.9	1.3	0.6	-	-	168	126
heart	23.7	0.7	103.0	1.4	87	0.76	0.15	3.2	0.6	2.0	1.7	9.3	12.7	124	71	43	3
colon	12.3	0.1	27.7	0.1	45	0.61	0.09	1.1	0.4	0.2	0.1	2.7	2.9	-	-	-	-
tongue	-	-	16.7	0.1	-	-	-	0.6	0.1	-	-	2.7	2.9	-	-	-	-
salivary gland	-	-	9.5	0.2	-	-	-	0.3	0.1	-	-	4.3	2.9	-	-	183	34
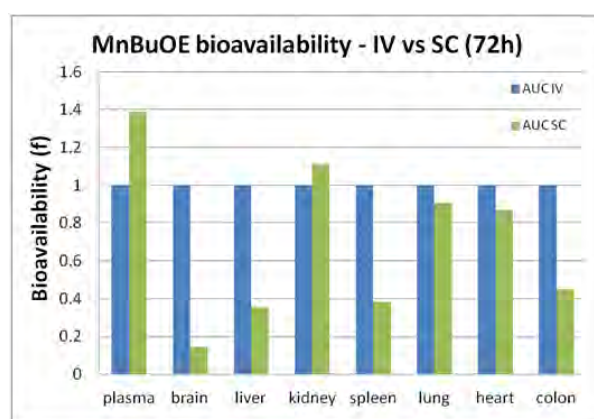
Figure 5. The 72-hour plasma and organ *sc* availability of MnTnBuOE-2-PyP^{5+} expressed relative to *iv* route. The values determined *via iv* route are taken as 100 % availability. Single injections of MnTnBuOE-2-PyP^{5+} were given *sc* at 10 mg/kg or *iv* at 2 mg/kg. Bioavailability after sc administration (*f*, or *F* when expressed as %) is defined as a ratio, AUC_{sc}/AUC_{iv}, normalized by dose, according to the equation: $f = 100 \times [(AUC_{sc} \times dose_{iv})/(AUC_{iv} \times dose_{sc})]$. AUC values relate to 72-hour period.

Multi-dosing long-term 56-day sc pharmacokinetic study. MnTnBuOE-2-PyP^{5+} was given as **(i)** a single injection **(ii)** once a week and **(iii)** every second week and at 4 doses of (a) 0.5 mg/kg; **(b)** 1 mg/kg**; (c)** 3 mg/kg and **(d)** 10 mg/kg. Drug levels were followed for 8 weeks, 56 days; frequency of analysis of MnP levels in plasma and organs is shown in **Figure 5**. The plasma was collected at 6 time points, while organs were analyzed at 2, 4 and 8 weeks. The PK curves are provided in **Figure 6** and the PK parameters calculated in **Table 3**.
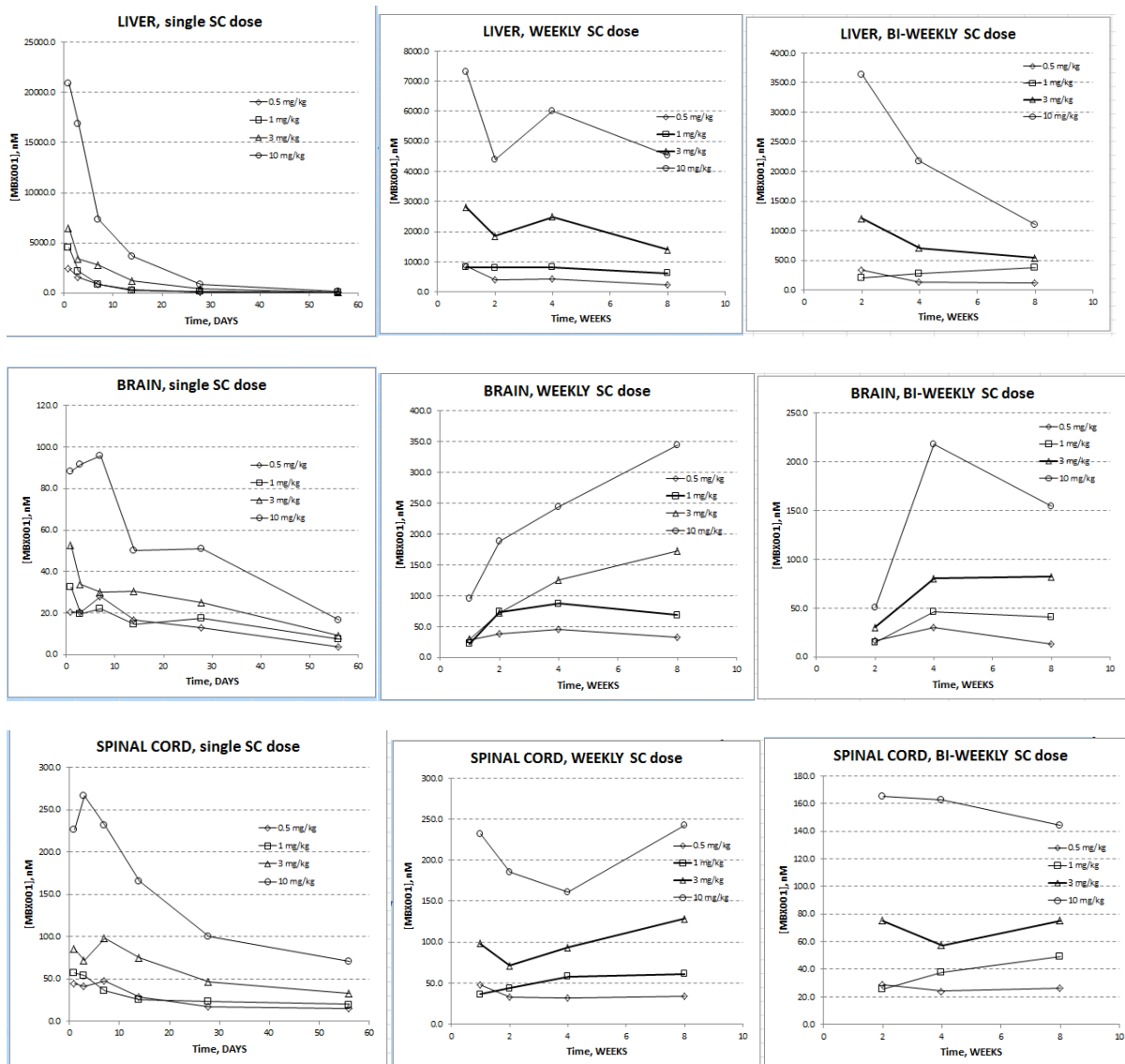
Figure 6. **The comprehensive *sc* PK study of MnTnBuOE-2-PyP^{5+}.** The MnP was given as a **(i)** single injection; **(ii)** once weekly; and **(iii)** once every second week (bi-weekly) and at several different doses: 0.5, 1, 3 and 10 mg/kg. MnP levels determined in plasma and in several organs at different time points. The organs to be analyzed were chosen in a way to cover studies where Mn porphyrins are explored in preclinical investigations (head and neck and brain tumors and central nervous system injuries). The PK data on salivary glands and tongue are provided in *Supplemental Material*, Figure S2.

Table 3. **The non-compartmental analysis of PK parameters for a single long-term 56 day *sc* PK study of MnTnBuOE-2-PyP^{5+}.**

Organ	Dose, mg/kg	AUC (1-56 days), day*µg/g	C_{max} (ng/g tissue)	t_{max} (days)	$t_{1/2}$ (28-56 day; d)	C at 56th day, ng/g tissue
Liver	0.5	22.9	3008	1	27	41
	1	29.2	5653	1	16	50
	3	71.4	8073	1	10	76
	10	226.5	26199	1	9	143
Brain	0.5	0.9	35	7	15	4
	1	1.1	41	1	23	10

	3	1.7	66	1	19	11
	10	3.5	120	7	17	21
Spinal cord	0.5	1.7	60	7	113	18
	1	1.8	71	1	120	25
	3	3.9	123	7	56	42
	10	9.1	333	3	54	88
Salivary gland	0.5	1.5	67	1	140	17
	1	1.7	132	1	107	19
	3	3.5	296	1	42	25
	10	9.6	817	1	27	48
Tongue	0.5	1.9	75	1	153	24
	1	2.2	108	1	100	26
	3	3.8	256	1	34	28
	10	8.3	573	1	25	37

The plasma and organ half-life, $t_{1/2}$, as well as AUC for 0.5 mg/kg *sc* 56-day dosing are shown in **Figure 7**. The highest availability was found in liver which serves as a drug reservoir to maintain stable levels of drug in other organs. We have chosen to concentrate on ≤ 1 mg/kg doses either given daily or every second day. Such doses are away from the multiple toxic doses which have been estimated for non-human primates in preliminary studies to be ≤ 6 mg/kg/day for 28 days. For comparison purposes the MnP distribution in different organs, in terms of AUC and $t_{1/2}$, are plotted in **Figure 7**. The values relate to 0.5 mg/kg 56-day single sc PK study. Based on $t_{1/2}$, the once-per-week dosing would maintain the stable MnP levels in organs.
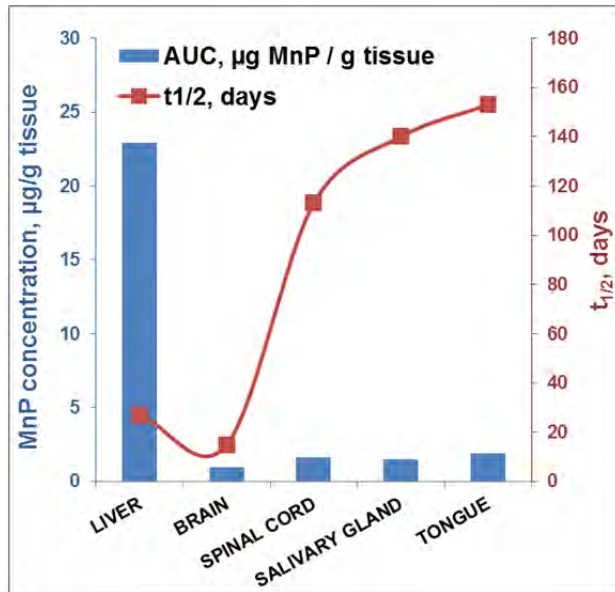

Figure 7. **The plasma and organ half-life, $t_{1/2}$, as well as AUC for 0.5 mg/kg *sc* 56-day single injection PK study of MnTnBuOE-2-PyP^{5+}**

Multi-dosing long-term 7-day and 28-day PK study. As compared to the 56-day PK study this study involved daily dosing over 7 and 28 days. Single dosing was conducted also. Mice were treated with single injection

at 4 different doses twice per day and for 7 and 28 days also. No loss in weight was demonstrated with all dosing schedules (Ashcraft et al, unpublished). Samples were taken at 12 hours after last injection to avoid the interference with high blood organ levels. The data related to plasma, liver and kidneys are shown in **Figure 8.** The data on other organs are shown in *Supplementary Material*. There is a constant accumulation of drug in all organs and saturation levels were not reached in any of the tissue analyzed.
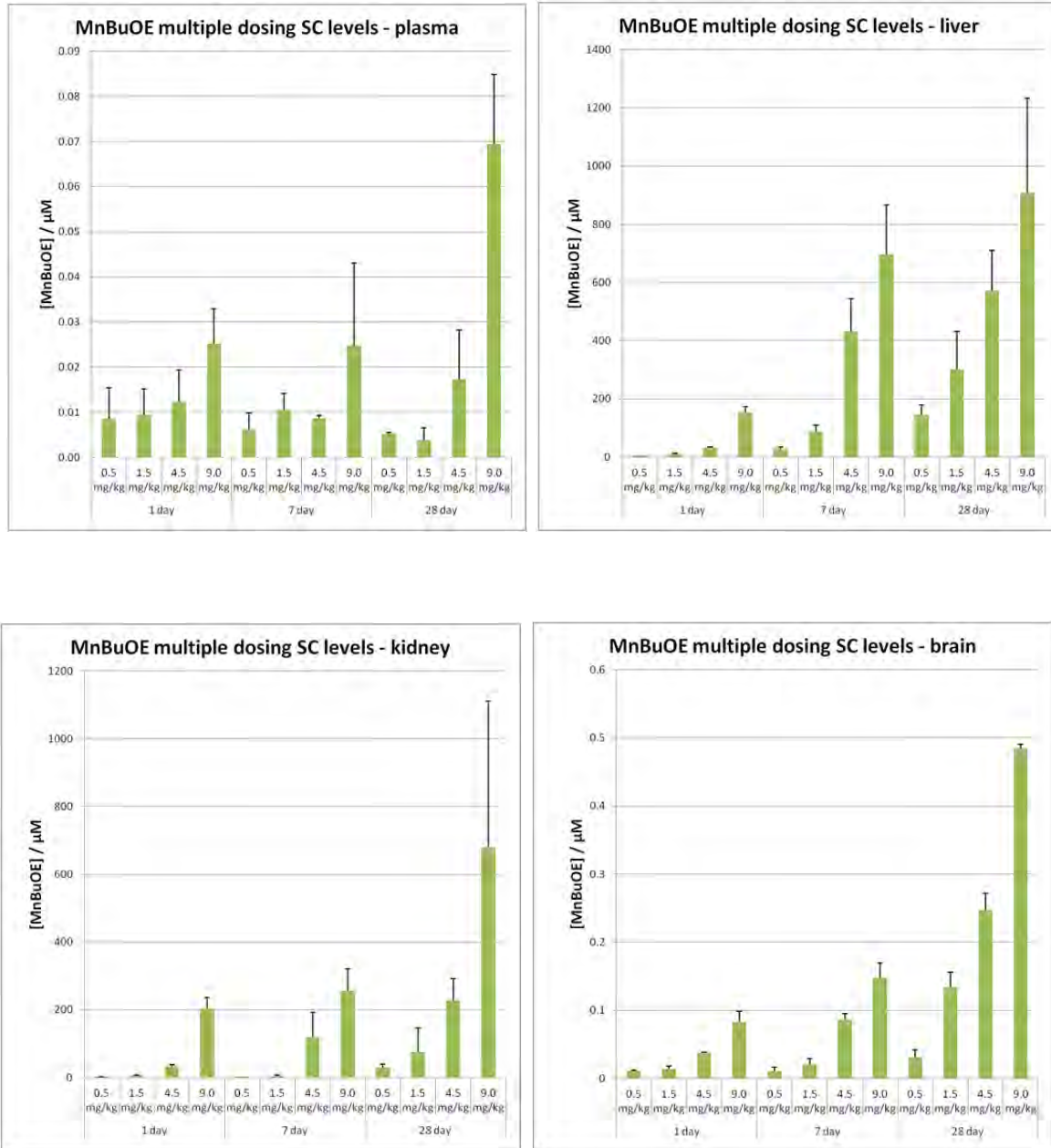
Figure 8. The accumulation of MnTnBuOE-2-PyP^{5+} in different organs after single injection (1 day), 7 days and 28 days dosing at 4 different doses given sc twice daily: 0.5, 1.5, 4.5 and 9 mg/kg. The samples were taken at 12 hours after last injection to minimize interference of the blood MnP with organ MnP levels. The MnP levels in plasma, liver, kidney and brain are given in micromoles per 1000mL plasma or tissue homogenate.

Reassessment of the oral availability of cationic Mn(III) N-substituted pyridylporphyrins. While experimental conditions were adjusted for the highest accuracy and precision, the possible significant impact of reflux in anesthetized mice supplied with artificial breathing onto MnP blood levels was overlooked when assessing MnP oral availibility. Consequently oral availability of cationic Mn(III) *N*-alkyl- and *N*-alkoxyalkylpyridylporphyrins was overestimated. We have here revisited their oral avilibility after failing to find the anticipated levels of Mn porphyrins when given either *via* oral gavage into the mouth cavity of awaken mouse, or as drinking water. The re-evaluation of the data sets oral avaibility of all 3 MnPs at ≥4%. The lowest value of 0.6% was found for most hydrophilic analog, MnTE-2-PyP^{5+}. However, our study opens the door to another excellent and facile route of their administration – inhalation. This exploration of this route of administration is particularly pertinent to the treatment of lung diseases.

Assessment of mouse perfusion prior to organ collection. We have routinely performed PK studies of MnPs in both plasma and organs. Thus far we have always perfused mice to assure that we have no contribution of plasma MnP's levels in their organ levels. This is particularly important when the levels of MnP in organs are assessed during first minutes up to 8 hours when MnP levels in plasma are still high. The issue, not earlier addressed, related to the possibility that perfusion forcefully clears the drug from intra- and extracellular space.

The perfusion vs non-perfusion experiment (**Figure 3)** was conducted at 7 day-time point. Relative to early time points, when MnP is still crossing the membranes and may localize to higher extent on the vessel walls, the MnP appears to be tightly bound inside cells/organs at day 7 post-injection. At that time point the perfusion does not affect levels of MnP as levels in plasma are lower than the lowest levels in organs. It is thus a safe strategy for anybody conducting PK studies to take organs at least 8 to 12 hours after last injection when levels in plasma are already low enough not to significantly affect organ levels and when MnP is presumably already within organs/cell and not on vessel walls.

At very early time points < 1 h, when plasma level are in high μM, and even though the mice were perfused, the data related to the organs (such as brain, **Figure 4**) with very low nM levels of porphyrins may be overstated and should be accounted for with caution.

Dosing of Mn porphyrins in preclinical studies. Appropriate dosing is crucial for the efficacy of any drug. Thus PK studies are essential to achieve maximal drug efficacy without compromising safety of animals and eventually humans. We have therefore conducted comprehensive PK studies herein and elsewhere in different animals and under different conditions [24, 28, 30, 32]. Based on such studies, it is obvious that Mn porphyrins exhibit a relatively slow clearance from all organs which allows for less frequent and patient-conveniently, once or twice weekly dosing, depending upon the targeted tissue. In most cases/organs one day is needed for MnP to peak;

thus whenever possible, the dosing should start at least 24 h before the oxidative-based injury. Different past and ongoing studies done on cells and animals [4, 10, 21, 33-35] suggest that more lipophilic drugs such as MnTnBuOE-2-PyP^{5+} and MnT nHex-2-PyP^{5+} are efficacious when administered at very low levels in the range of 0.1 to 1 mg/kg. The less lipophilic drugs, such MnTE-2-PyP^{5+} (and its methyl *ortho* and methyl and ethyl *meta* analogs) should be dosed at concentrations ≥ 5 mg/kg. The safety/toxicity profiles of MnPs are very much dependent upon their lipophilicities/accumulation which differ several orders of magnitude going from MnTM-2-PyP^{5+} over MnTnHex-2-PyP^{5+} to MnTnBuOe-2-PyP^{5+} [4, 5, 33, 36]. Based on our accumulation and mechanistic studies [5, 37] the more lipophilic compounds incorporate to a higher extent within membranes where they compromise their integrity. In addition their redox-properties play a role as non-redox-active Zn analogs are not toxic though they incorporate in membranes to similar levels driven by the nature of alkyl substituents on pyridyl nitrogens [3, 37-39]. With certain conditions, such as stroke, where fast accumulation in brain is required, *iv* route may be preferred. However, Mn porphyrins cause significant dose-dependent blood pressure drop (BPD) when given *via iv* route, and more so lipophilic analogs [40]. Therefore, *sc* route of administration (where BPD was much less expressed), though inferior with regards to the speed of CNS system delivery, is preferred whenever possible, as it still affords fairly fast delivery of MnP into all organs, and a large body exposure to MnP, AUC.

Acknowledgement

Abbreviations

$E_{1/2}$, half-wave reduction potential; SOD, superoxide dismutase; $k_{cat}(O_2^{\cdot-})$, rate constant for the catalysis of $O_2^{\cdot-}$ dismutation by MnP; NHE, normal hydrogen electrode; P_{OW}, partition coefficient between n-octanol and water; $ONOO^-$, peroxynitrite; $O_2^{\cdot-}$, superoxide; ClO^-, deprotonated hypochlorite; MnTE-2-PyP^{5+}, AEOL10113, Mn(III) *meso*-tetrakis(*N*-ethylpyridinum-2-yl)porphyrin; MnTnHex-2-PyP^{5+}, Mn(III) *meso*-tetrakis(*N*-n-hexylpyridinum-2-yl)porphyrin; MnTnBuOE-2-PyP^{5+}, Mn(III) *meso*-tetrakis(*N*-n-butoxyethyllpyridinum-2-yl)porphyrin, BMX-001; PK, pharmacokinetics, AUC, are under curve; $t_{1/2}$, half-life; C_{max}, maximal concentration; C_{24}, concentration at 24 h; *ip*, intraperitoneal; *iv,* intravenous; *sc*; subcutaneous.

References

[1]   Spasojevic, I.; Miryala, S.; Tovmasyan, A.; Salvemini, D.; Vujaskovic, Z.; Batinic-Haberle, I.; St. Clair, D. Lipophilicity of Mn(III) *N*-alkylpyridylporphyrins dominates their accumulation within mitochondria and therefore *in vivo* efficacy. A mouse study. *Free Radic Biol Med* **51:**S98; 2011.

[2]   Spasojevic, I.; Weitner, T.; Tovmasyan, A.; Sheng, H.; Miriyala, S.; Leu, D.; Rajic, Z.; Warner, D. S.; Clair, D. K.; Huang, T. T.; Batinic-Haberle, I. Pharmacokinetics, Brain Hippocampus and Cortex, and Mitochondrial Accumulation of a New Generation of Lipophilic Redox-Active Therapeutic, Mn(III) *Meso* Tetrakis(*N*-n-butoxyethylpyridinium-2-yl)porphyrin, MnTnBuOE-2-PyP^{5+}, in Comparison with its Ethyl and N-hexyl Analogs, MnTE-2-PyP^{5+} and MnTnHex-2-PyP^{5+}. *Free Rad Biol Med* **65:**S132; 2013.

[3]   Batinic-Haberle, I.; Tovmasyan, A.; Roberts, E. R.; Vujaskovic, Z.; Leong, K. W.; Spasojevic, I. SOD Therapeutics: Latest Insights into Their Structure-Activity Relationships and Impact on the Cellular Redox-Based Signaling Pathways. *Antioxid Redox Signal* **20:**2372-2415; 2014.

[4]   Rajic, Z.; Tovmasyan, A.; Spasojevic, I.; Sheng, H.; Lu, M.; Li, A. M.; Gralla, E. B.; Warner, D. S.; Benov, L.; Batinic-Haberle, I. A new SOD mimic, Mn(III) ortho N-butoxyethylpyridylporphyrin, combines superb potency and lipophilicity with low toxicity. *Free Radic Biol Med* **52:**1828-1834; 2012.

[5]   Tovmasyan, A.; Reboucas, J. S.; Benov, L. Simple biological systems for assessing the activity of superoxide dismutase mimics. *Antioxid Redox Signal* **20:**2416-2436; 2014.

[6]   Weitzel D, A. K., Liu C, Li W, Buckley A, Rodriguiz RM, Wetsel WC, Spasojevic I, Tovmasyan A, Peters KB, Batinic-Haberle I, Dewhirst MW. Radioprotection of brain white matter by the catalytic MnSOD mimic / antioxidant, BMX-001. *Pediatric Neuro-Oncology Basic and Translational Research Conference*. Ft. Lauderdale, Florida; 2013.

[7]   Miriyala, S.; Spasojevic, I.; Tovmasyan, A.; Salvemini, D.; Vujaskovic, Z.; St Clair, D.; Batinic-Haberle, I. Manganese superoxide dismutase, MnSOD and its mimics. *Biochim Biophys Acta* **1822:**794-814; 2012.

[8]   Holley, A. K.; Xu, Y.; Noel, T.; Bakthavatchalu, V.; Batinic-Haberle, I.; St Clair, D. K. Manganese Superoxide Dismutase-Mediated Inside-Out Signaling In HaCaT Human Keratinocytes and SKH-1 Mouse Skin. *Antioxid Redox Signal*; 2014.

[9]   Zhao, Y.; Miriyala, S.; Miao, L.; Mitov, M.; Schnell, D.; Dhar, S. K.; Cai, J.; Klein, J. B.; Sultana, R.; Butterfield, D. A.; Vore, M.; Batinic-Haberle, I.; Bondada, S.; St. Clair, D. K. Redox Proteomic identification of HNE-bound mitochondrial proteins in cardiac tissues reveals a systemic effect on energy metabolism after Doxorubicin treatment. *Free Radic Biol Med* **In revision**; 2014.

[10]   Weitzel, D. H.; Tovmasyan, A.; Ashcraft, K. A.; Rajic, Z.; Weitner, T.; Liu, C.; Li, W.; Buckley, A. F.; Prasad, M. R.; Young, K. H.; Rodriguiz, R. M.; Wetsel, W. C.; Peters, K. B.; Spasojevic, I.; Herndon II, J. I.; Batinic-Haberle, I.; Dewhirst, M. W. Radioprotection of the brain white matter by Mn(III) N-butoxyethylpyridylporphyrin-based superoxide dismutase mimic, MnTnBuOE-2-PyP5+. *Mol Cancer Ther* **In Revision**; 2014.

[11]   Leu, D.; Zou, Y.; Weitner, T.; Tovmasyan, A.; Spasojevic, I.; Batinic-Haberle, I.; Huang, T.-T. Radiation protection of hippocampal neurogenesis with Mn-containing porphyrins. *The 60th Annual Meeting of the Radiation Research Society* Las Vegas, Nevada, USA; 2014.

[12]   Ashcraft, K. A.; Palmer, G.; Spasojevic, I.; Batinic-Haberle, I.; Dewhirst, M. W. Radioprotection of the salivary gland and oral mucosa with a novel porphyrin-based antioxidant. *58th Annual Meeting of the Radiation Research Society***:**129; 2012.

[13]   Jaramillo, M. C.; Briehl, M. M.; Crapo, J. D.; Batinic-Haberle, I.; Tome, M. E. Manganese porphyrin, MnTE-2-PyP5+, Acts as a pro-oxidant to potentiate glucocorticoid-induced apoptosis in lymphoma cells. *Free Radic Biol Med* **52:**1272-1284; 2012.

[14]   Jaramillo, M. C.; Frye, J. B.; Crapo, J. D.; Briehl, M. M.; Tome, M. E. Increased manganese superoxide dismutase expression or treatment with manganese porphyrin potentiates dexamethasone-induced apoptosis in lymphoma cells. *Cancer Res* **69:**5450-5457; 2009.

---

[15]   Tovmasyan, A.; Weitner, T.; Jaramillo, M.; Wedmann, R.; Roberts, E.; Leong, K. W.; Filipovic, M.; Ivanovic-Burmazovic, I.; Benov, L.; Tome, M.; Batinic-Haberle, I. We have come a long way with Mn porphyrins: from superoxide dismutation to H_2O_2-driven pathways. *Free Rad Biol Med* **65:**S133; 2013.

[16]   Tovmasyan, A.; Weitner, T.; Roberts, E.; Jaramillo, M.; Spasojevic, I.; Leong, K.; Tome, M.; Benov, L.; Batinic-Haberle, I. Understanding differences in mechanisms of action of Fe vs Mn porphyrins: comparison of their reactivities towards cellular reductants and reactive species. *Free Radic Biol Med* **53:**S120; 2012.

[17]   Evans, M. K.; Tovmasyan, A.; Batinic-Haberle, I.; Devi, G. R. Mn porphyrin in combination with ascorbate acts as a pro-oxidant and mediates caspase-independent cancer cell death. *Free Radic Biol Med* **68:**302-314; 2014.

[18]   Ye, X.; Fels, D.; Tovmasyan, A.; Aird, K. M.; Dedeugd, C.; Allensworth, J. L.; Kos, I.; Park, W.; Spasojevic, I.; Devi, G. R.; Dewhirst, M. W.; Leong, K. W.; Batinic-Haberle, I. Cytotoxic effects of Mn(III) N-alkylpyridylporphyrins in the presence of cellular reductant, ascorbate. *Free Radic Res* **45:**1289-1306; 2011.

[19]   Rawal, M.; Schroeder, S. R.; Wagner, B. A.; Cushing, C. M.; Welsh, J. L.; Button, A. M.; Du, J.; Sibenaller, Z. A.; Buettner, G. R.; Cullen, J. J. Manganoporphyrins Increase Ascorbate-Induced Cytotoxicity by Enhancing H2O2 Generation. *Cancer Res* **73:**5232-5241; 2013.

[20]   Oberley-Deegan, R. E.; Steffan, J. J.; Rove, K. O.; Pate, K. M.; Weaver, M. W.; Spasojevic, I.; Frederick, B.; Raben, D.; Meacham, R. B.; Crapo, J. D.; Koul, H. K. The Antioxidant, MnTE-2-PyP, Prevents Side-Effects Incurred by Prostate Cancer Irradiation. *PLoS One* **7:**e44178; 2012.

[21]   Batinic-Haberle, I.; Ndengele, M. M.; Cuzzocrea, S.; Reboucas, J. S.; Spasojevic, I.; Salvemini, D. Lipophilicity is a critical parameter that dominates the efficacy of metalloporphyrins in blocking the development of morphine antinociceptive tolerance through peroxynitrite-mediated pathways. *Free Radic Biol Med* **46:**212-219; 2009.

[22]   Liu, T.; Ji, R. R. Oxidative stress induces itch via activation of transient receptor potential subtype ankyrin 1 in mice. *Neurosci Bull* **28:**145-154; 2012.

[23]   Jumbo-Lucioni, P. P.; Ryan, E. L.; Hopson, M. L.; Bishop, H. M.; Weitner, T.; Tovmasyan, A.; Spasojevic, I.; Batinic-Haberle, I.; Liang, Y.; Jones, D. P.; Fridovich-Keil, J. L. Manganese-Based Superoxide Dismutase Mimics Modify Both Acute and Long-Term Outcome Severity in a Drosophila melanogaster Model of Classic Galactosemia. *Antioxid Redox Signal* **20:**2361-2371; 2014.

[24]   Weitner, T.; Kos, I.; Sheng, H.; Tovmasyan, A.; Reboucas, J. S.; Fan, P.; Warner, D. S.; Vujaskovic, Z.; Batinic-Haberle, I.; Spasojevic, I. Comprehensive pharmacokinetic studies and oral bioavailability of two Mn porphyrin-based SOD mimics, MnTE-2-PyP(5+) and MnTnHex-2-PyP(5+). *Free Radic Biol Med* **58:**73-80; 2013.

[25]   Batinić-Haberle, I.; Spasojević, I.; Stevens, R. D.; Hambright, P.; Fridovich, I. Manganese(III) *meso*-tetrakis(*ortho-N*-alkylpyridyl)porphyrins. Synthesis, characterization, and catalysis of $O_2^{\cdot-}$ dismutation. *J. Chem. Soc., Dalton Trans.*:2689-2696; 2002.

[26]   Kos, I.; Reboucas, J. S.; DeFreitas-Silva, G.; Salvemini, D.; Vujaskovic, Z.; Dewhirst, M. W.; Spasojevic, I.; Batinic-Haberle, I. Lipophilicity of potent porphyrin-based antioxidants: comparison of ortho and meta isomers of Mn(III) N-alkylpyridylporphyrins. *Free Radic Biol Med* **47:**72-78; 2009.

[27]   Spasojevic, I.; Menzeleev, R.; White, P. S.; Fridovich, I. Rotational isomers of N-alkylpyridylporphyrins and their metal complexes. HPLC separation, H-1 NMR and X-ray structural characterization, electrochemistry, and catalysis of O-2(center dot-) disproportionation. *Inorganic Chemistry* **41:**5874-5881; 2002.

[28]   Spasojevic, I.; Li, A.; Tovmasyan, A.; Rajic, Z.; Salvemini, D.; St Clair, D.; Valentine, J. S.; Vujaskovic, Z.; Gralla, E. B.; Batinic-Haberle, I. Accumulation of Porphyrin-based SOD Mimics in Mitochondria is Proportional to Their Lipophilicity: S-cerevisiae Study of ortho Mn(III) N-alkylpyridylporphyrins. *Free Radic Biol Med* **49:**S199-S199; 2010.

[29]   Rausaria, S.; Ghaffari, M. M.; Kamadulski, A.; Rodgers, K.; Bryant, L.; Chen, Z.; Doyle, T.; Shaw, M. J.; Salvemini, D.; Neumann, W. L. Retooling manganese(III) porphyrin-based peroxynitrite decomposition catalysts for selectivity and oral activity: a potential new strategy for treating chronic pain. *J Med Chem* **54:**8658-8669; 2011.

[30]   Spasojevic, I.; Chen, Y.; Noel, T. J.; Fan, P.; Zhang, L.; Reboucas, J. S.; St Clair, D. K.; Batinic-Haberle, I. Pharmacokinetics of the potent redox-modulating manganese porphyrin, MnTE-2-PyP(5+), in plasma and major organs of B6C3F1 mice. *Free Radic Biol Med* **45:**943-949; 2008.

[31]   Spasojevic, I.; Chen, Y.; Noel, T. J.; Yu, Y.; Cole, M. P.; Zhang, L.; Zhao, Y.; St Clair, D. K.; Batinic-Haberle, I. Mn porphyrin-based superoxide dismutase (SOD) mimic, MnIIITE-2-PyP5+, targets mouse heart mitochondria. *Free Radic Biol Med* **42:**1193-1200; 2007.

[32]   Spasojevic, I.; Kos, I.; Benov, L. T.; Rajic, Z.; Fels, D.; Dedeugd, C.; Ye, X.; Vujaskovic, Z.; Reboucas, J. S.; Leong, K. W.; Dewhirst, M. W.; Batinic-Haberle, I. Bioavailability of metalloporphyrin-based SOD mimics is greatly influenced by a single charge residing on a Mn site. *Free Radic Res* **45:**188-200; 2011.

[33]   Kos, I.; Benov, L.; Spasojevic, I.; Reboucas, J. S.; Batinic-Haberle, I. High lipophilicity of meta Mn(III) N-alkylpyridylporphyrin-based superoxide dismutase mimics compensates for their lower antioxidant potency and makes them as effective as ortho analogues in protecting superoxide dismutase-deficient Escherichia coli. *J Med Chem* **52:**7868-7872; 2009.

[34]   Miriyala, S.; Thippakorn, C.; Chaiswing, L.; Xu, Y.; Noel, T.; Tovmasyan, A.; Batinic-Haberle, I.; Kooi, C. V.; Chi, W.; Latif, A. A.; Reda, H.; Oberley, T.; Prachayasittikul, V.; Clair, D. K. 4-hydroxy-2-nonenal triggers AIFM2-mediated retrograde signaling by activating its translocation and function switching. *Submitted*; 2013.

[35]   Sheng, H.; Spasojevic, I.; Tse, H. M.; Jung, J. Y.; Hong, J.; Zhang, Z.; Piganelli, J. D.; Batinic-Haberle, I.; Warner, D. S. Neuroprotective Efficacy from a Lipophilic Redox-Modulating Mn(III) N-Hexylpyridylporphyrin, MnTnHex-2-PyP: Rodent Models of Ischemic Stroke and Subarachnoid Hemorrhage. *J Pharmacol Exp Ther* **338:**906-916; 2011.

[36]   Tovmasyan, A. G.; Rajic, Z.; Spasojevic, I.; Reboucas, J. S.; Chen, X.; Salvemini, D.; Sheng, H.; Warner, D. S.; Benov, L.; Batinic-Haberle, I. Methoxy-derivatization of alkyl chains increases the in vivo efficacy of cationic Mn porphyrins. Synthesis, characterization, SOD-like activity, and SOD-deficient E. coli study of meta Mn(III) N-methoxyalkylpyridylporphyrins. *Dalton Trans* **40:**4111-4121; 2011.

[37]   Ezzeddine, R.; Al-Banaw, A.; Tovmasyan, A.; Craik, J. D.; Batinic-Haberle, I.; Benov, L. T. Effect of molecular characteristics on cellular uptake, subcellular localization, and phototoxicity of Zn(II) N-alkylpyridylporphyrins. *J Biol Chem* **288:**36579-36588; 2013.

[38]   Batinic-Haberle, I.; Spasojevic, I.; Tse, H. M.; Tovmasyan, A.; Rajic, Z.; St Clair, D. K.; Vujaskovic, Z.; Dewhirst, M. W.; Piganelli, J. D. Design of Mn porphyrins for treating oxidative stress injuries and their redox-based regulation of cellular transcriptional activities. *Amino Acids* **42:**95-113; 2012.

[39]   Benov, L.; Craik, J.; Batinic-Haberle, I. Protein damage by photo-activated Zn(II) N-alkylpyridylporphyrins. *Amino Acids* **42:**117-128; 2012.

[40]   Ross, A. D.; Sheng, H.; Warner, D. S.; Piantadosi, C. A.; Batinic-Haberle, I.; Day, B. J.; Crapo, J. D. Hemodynamic effects of metalloporphyrin catalytic antioxidants: structure-activity relationships and species specificity. *Free Radic Biol Med* **33:**1657-1669; 2002.